Hindawi
Wireless Communications and Mobile Computing
Volume 2018, Article ID 9715428, 23 pages
https://doi.org/10.1155/2018/9715428

Research Article

Green Data Gathering under Delay Differentiated Services Constraint for Internet of Things

Mingfeng Huang,[1] Anfeng Liu ,[1] Tian Wang,[2] and Changqin Huang[3]

[1]*School of Information Science and Engineering, Central South University, Changsha 410083, China*
[2]*School of Computer Science, National Huaqiao University, Quanzhou 362000, China*
[3]*School of Information Technology in Education, South China Normal University, Guangzhou 510631, China*

Correspondence should be addressed to Anfeng Liu; afengliu@mail.csu.edu.cn

Received 22 August 2017; Revised 4 December 2017; Accepted 19 December 2017; Published 26 February 2018

Academic Editor: Zhi Liu

Energy-efficient data gathering techniques play a crucial role in promoting the development of smart portable devices as well as smart sensor devices based Internet of Things (IoT). For data gathering, different applications require different delay constraints; therefore, a delay Differentiated Services based Data Routing (DSDR) scheme is creatively proposed to improve the delay differentiated services constraint that is missed from previous data gathering studies. The DSDR scheme has three advantages: first, DSDR greatly reduces transmission delay by establishing energy-efficient routing paths (E2RPs). Multiple E2RPs are established in different locations of the network to forward data, and the duty cycles of nodes on E2RPs are increased to 1, so the data is forwarded by E2RPs without the existence of sleeping delay, which greatly reduces transmission latency. Secondly, DSDR intelligently chooses transmission method according to data urgency: the direct-forwarding strategy is adopted for delay-sensitive data to ensure minimum end-to-end delay, while wait-forwarding method is adopted for delay-tolerant data to perform data fusion for reducing energy consumption. Finally, DSDR make full use of the residual energy and improve the effective energy utilization. The E2RPs are built in the region with adequate residual energy and they are periodically rotated to equalize the energy consumption of the network. A comprehensive performance analysis demonstrates that the DSDR scheme has obvious advantages in improving network performance compared to previous studies: it reduces transmission latency of delay-sensitive data by 44.31%, reduces transmission latency of delay-tolerant data by 25.65%, and improves network energy utilization by 30.61%, while also guaranteeing the network lifetime is not lower than previous studies.

1. Introduction

Internet of Things (IoT) [1–3] and cloud computing [4–6] leverage the ubiquity of sensor-equipped devices (e.g., smart portable devices, smart sensor nodes) to collect information at low cost and provide a new paradigm for solving the complex sensing applications from the significant demands of critical infrastructure such as surveillance systems [7–10], remote patient care systems in healthcare [11, 12], intelligent traffic management [13], automated vehicles in transportation environmental [14], and weather monitoring systems. Data gathering is one of the important functions for such sensor based networks, in which each smart sensor based device is sensing information from the surrounding environment and sends data to the sink via multihop routing. After data have been acquired, the sink can make decisions about perceived events, thus bringing smart life to people [8, 10, 11]. But, due to the limited energy of sensor devices, how to ensure that data is gathered to the sink quickly as well as in an energy-efficient way is an important issue [15–17].

Although the smart sensor based devices (e.g., wireless sensor nodes, smart phone, and tablets) have powerful computing and communication capabilities, the data produced are getting more and more as the scope of application expands and the variety increases, so the energy of the device is drained out much faster than before. Green communications play a critical role in or are expected to be an indispensable part of the smart sensor based networks [1, 10, 13, 18]. Due to the diversity and complexity of applications running over the networks, green communications under delay or quality of

service guarantee in such networks gain increasing attention in the research community [19, 20] and face a great challenge.

(1) The challenge of green communication: communication consumption is the largest energy consumption in sensor based networks, so the key to green communications is to effectively reduce the energy consumption in communication. Overall, the main ways to reduce energy consumption are as follows:

(a) Using asynchronous sleep/waking working mode can effectively reduce the energy consumption of nodes. In this mode, the sensor nodes periodically rotate between sleeping and waking states, and the ratio of the duration that the nodes are in the waking state to the unit cycle is called the duty cycle [11, 21]. In general, the energy consumption of the node in the sleeping state is 1/100–1/1000 of that in waking state [8, 12, 21]; thus, in order to save energy, the node should be in sleeping state as much as possible. However, the node can communicate only when it is in waking state, so the small duty cycle of node can reduce its energy consumption effectively, but when it has data to send, it needs to wait for the waking up of the receiver to communicate. And the time required from the preparation of data at the sender to the waking up at the receiver is called sleeping delay. This means that to reduce the data transmission delay it is necessary to increase the duty cycle, but at the same time it will increase the energy consumption of the node, so how to balance the delay and energy consumption is a tricky problem.

(b) Another way to effectively reduce energy consumption is data fusion. Reference [22] points out that event information has relevance both in time and in space, so data fusion can be used to fuse multiple event information, thus greatly reducing the amount of data and reducing energy consumption. From the perspective of reducing energy consumption, more data packets should be fused so that the redundancy is minimized. Although a lot of routing strategies for data fusion have been proposed, most of them have not been applied to sensor networks. What is more, applications often require that the delay of the data's arrival is less than a specified threshold. For example, in a fire monitoring system, "alarm" message is required to be transmitted to the control center as soon as possible; otherwise it will cause significant losses. The same situation exists in the medical systems, the sensor node attached to the patient is generally used to record the patient's daily vital signs, but, in an emergency where the patient's heart rate changes dramatically, the "alarm" packet of the data needs to be transmitted to the doctor in time to take the appropriate first-aid measures [5, 12, 23]. Obviously, in such cases, the strategies proposed for maximizing data fusion are not able to ensure that the delay satisfies the requirements. Therefore, it is another important issue to make the data fusion under the precondition of guaranteeing the application delay and reduce the network energy consumption effectively.

(2) The delay or quality of service (QoS) guarantees for sensor networks: as an important part of information infrastructure, sensor based networks often collect data for a variety of applications. Different applications have different requirements for QoS, and even the same applications may have different requirements due to the different events [20, 22], where delay is the basic metrics in data gathering. Generally speaking, delay-sensitive data requires a small delay to the sink, and delay-tolerant data can tolerate a certain delay. The best way to optimize network performance is to use a differentiated service to distinguish different transmissions to meet application requirements. But, to the best of our knowledge, there is no research that is able to provide differentiated services in green communications.

In summary, how to combine the settings of duty cycles with data fusion technologies and differentiated services to establish efficient routings to ensure energy-efficient and delay-guaranteed data gathering is of great significance and also has broad application prospects. Thus, a delay Differentiated Services based Data Routing (DSDR) scheme is creatively proposed, in which the energy consumption can be reduced and delay can be guaranteed for applications. The contributions of the DSDR scheme are as follows.

(1) The DSDR scheme has high energy efficiency and reduces transmission delay greatly by establishing energy-efficient routing paths (E2RPs). First, multiple E2RPs are established in different locations of the network to forward data, and the duty cycles of nodes on E2RPs are increased to 1, so the data is forwarded by E2RPs without the existence of sleeping delay, which greatly reduces transmission latency. What is more, the E2RPs are built in the region with adequate residual energy, and the residual energy of nodes on E2RPs is periodically measured, and once the remaining energy is below the threshold, the E2RP where the node located is immediately removed. Therefore, the DSDR scheme enhances the energy utilization of network effectively without affecting the network lifetime.

(2) The DSDR scheme adopts delay differentiated services, which makes the scheme have a better performance under the premise of guaranteeing the service quality. In DSDR, for delay-sensitive data, the direct-forwarding strategy is used to ensure the minimal end-to-end transmission delay, while, for delay-tolerant data, the wait-forwarding method and data fusion are adopted to reduce energy consumption.

(3) The DSDR scheme has the capability of global event data fusion, which greatly reduces the data amount needed

to be transmitted and improves the energy efficiency of the network. Firstly, E2RPs are naturally data fusion paths, which can greatly increase the probability of data fusion. Secondly, the data are all routed through E2RPs, making the data fusion under DSDR scheme global and the largest possible, which greatly reduces data redundancy and energy consumption. To the best of our knowledge, the DSDR is the first more perfect combination of data fusion, differentiated services, and duty cycle setting and integrates an efficient data gathering in a number of performances far better than the previous studies.

(4) Through our extensive theoretical analysis, we demonstrate that the DSDR scheme proposed in this paper has better performances. It realizes synchronous optimization in latency and energy, reduces the transmission delay of delay-sensitive data by 44.31%, reduces the transmission delay of delay-tolerant data by 25.65%, and improves network energy utilization by 30.61%. Compared with the previous schemes, DSDR has obvious advantages in delay optimization and energy utilization.

The rest of this paper is organized as follows: in Section 2, a literature review related to this work is introduced. Then the system model and problem statement are described in Section 3. In Section 4, we proposed an efficient DSDR scheme. The performance analysis of the DSDR scheme is provided in Section 5. Finally, Section 6 presented the conclusion and future perspectives of our work.

2. Related Work

Different applications running on the same network platform may have different requirements on the service of quality; the basic requirement is network delay [19, 21, 24, 25]. In this section, we introduce some state-of-the-art researches for delay differentiated service.

Considering the network delay simply, the duty cycle is the key to reduce delay [26–29]. In WSNs, the node is awake periodically; the longer the node in the waking state, the smaller its sleeping delay, and the smaller the network latency. Based on this idea, the authors of [14] proposed a distributed duty cycle allocation algorithm. The algorithm uses the network residual energy to gradually increase the duty cycles of nodes in the far-sink region based on the distance between the node and the sink and makes the delay of the network external nodes decrease. In [16], the authors also consider the adjustment of the node duty cycle. However, the adjustment under this study is based on the load of the entire network. This kind of duty cycle adjustment scheme has some innovation, but it increases the complexity of the network system, especially when the network is large and the parameter configuration will be tricky.

In addition, since the data are transmitted to the sink through multihop relays, reducing the hops of relay can effectively reduce the end-to-end delay. The authors of [15] realize this and propose a communication scheme called T-LOGF to select the next hop based on the shortest distance. The scheme uses one-step-look-ahead data transmission principle, each time selects the node with the smallest distance from the sink to forward data, so that the total relay hops can be minimized, and reduces the delay, but the scheme ignores the waiting delay caused by the sleep/waking mode.

In [30], the authors studied the issue of network latency requirements for differential services in content-centric networking (CCN), while optimizing the content overall transmission performance. In this paper, in order to guarantee the network delay, the authors first proposed a simple and comprehensive network model; the network delay of routing content is characterized to different locations of the client. Ensure that each content provider has optimized content and latency by combining network locations with content popularity. Then, the content distribution model is incorporated into the proposed global network model, and the delay is addressed as the nonlinear integer programming (NIP) problem in the given network resource and traffic access mode.

The above studies have been considered unilaterally from the network latency, but in fact the data integrity is valued by most applications. In [3], a multipath dynamic routing algorithm called IDDR is proposed to satisfy these two requirements simultaneously. In IDDR, according to the sensitivity of the data to delay and integrity, on the basis of weights of each packet and different QoS requirements, the data packets in the network are separated, and different data are transferred to the sink through different paths to improve data fidelity and integrity and minimize the end-to-end transmission latency. This dynamic routing for data integrity and delay differentiated service can meet the quality requirements of different data, but it is necessary to create a route for each data transfer, increasing the complexity of the network.

Similar to [3], authors of [31] evaluate the quality of the network from the timeliness and reliability. The authors proposed a packet delivery mechanism called Multipath and Multi-SPEED Routing Protocol (MMSPEED) to improve data latency and reliability. For timeliness, MMSPEED provides multiple QoS levels to ensure the transmission speed of multiple packets. For reliability, probabilistic multipath forwarding supports the various reliability requirements of data. These mechanisms for QoS provisioning are realized in a localized way without global information by adopting localized geographic packet forwarding augmented with dynamic compensation, which compensates for local decision inaccuracies as a packet travels towards the destination.

In a more complex system, the quality of service of the network may involve multiple parameters [32–36]. In [20], the authors proposed RPL for the application of traffic prioritization and differentiation for bandwidth, delay, reliability, and security. RPL addresses QoS channel access through queue scheduling mechanism or the priority of media access control (MAC). Specifically, multiple instances of RPL implement the validity of QoS differences based on different objective functions. At the same time, three variants of RPL: standard RPL, multi-instance RPL (RPL-M), and multi-instance RPL with prioritized channel backoffs (RPL-M+) along with two distinct traffic classes have been examined as data traffic rate and composition was varied.

A three-layer QoS scheduling model is proposed for service-oriented IoT in [37]; it selects different scheduling

schemes from the application layer, network layer, and sensing layer. In application layer, it uses the service of each component to explore the best QoS-aware service composition. In network layer, the model mainly deals with the scheduling of a heterogeneous network environment. In sensing layer, it is responsible for different service information collection and resource allocation scheduling. The scheme can reduce the costs of network resources in a certain extent.

WSNs are highly complex systems, and energy consumption in resource-constrained WSNs is also an important parameter to consider when reducing network latency. In-network data fusion and clustering are important technologies to reduce energy consumption in wireless sensor networks; the authors of [38] proposed a delay-aware network structure for WSNS with in-network data fusion by utilizing this technique, which divides the sensor nodes into different size clusters, so that each cluster can communicate with the fusion center in an interleaved manner. At the same time, an optimization process is proposed to optimize the communication distance within the group. The proposed network can reduce the latency of the data aggregation process, provided that the data can only be partially fused.

Villas et al. of [22] also use data fusion to achieve the performance requirements of the network and propose an in-network data aggregation routing strategy. The strategy establishes routing paths in the nonhotspot area of the network, and then a number of events that occur in different area are merged into the path, and when the packets of these events go through the same node, data fusion is performed to reduce redundancy. However, this strategy can only be part of the local event information together, but no global network event information fusion capabilities.

In relatively differentiated services, the network traffic is divided into a small number of service classes based on their packets transmission quality, in terms of per-hop metrics for queuing delays and packet losses. In [39], the authors improved and quantified relatively differentiated services and proposed proportional differentiation model for network operators providing "tuning knobs" to adjust the quality interval between classes. The model has a strict priority or capacity differentiation and does not consider the class load and loss differences.

It can be seen from the above that duty cycle and data fusion are all key technologies to improve network performance. Therefore, in the DSDR scheme, we first reduce the transmission delay of delay-sensitive data by increasing duty cycles of relay nodes and then decrease the energy consumption of delay-tolerant data by data fusion.

3. The System Model and Problem Statement

3.1. System Model. The network model of this paper is a typical planar periodic data gathering wireless sensor network, which is similar to [14, 40]; its model structure is as follows.

(1) N homogeneous sensor nodes are randomly deployed in a two-dimensional planar network, the sink is the center of the entire network, the network radius is R, the node communication radius is r, and the node density is ρ. Each node in the network continuously monitors the surrounding environment, and once the event of interest is detected, the event data is immediately sent to the sink via multihop relays.

(2) Sensor nodes sleep/waking work periodically, nodes monitor the target and transmit the data in the waking state. All the monitoring targets are randomly distributed in different positions of the network, so the probability that each node monitors target and generates data is equal.

(3) The lossless step-by-step multihop aggregation model is used in this paper [22]. In this model, the result of data fusion of nodes ς_i and ς_j is denoted by $\Gamma_{\varsigma_i\varsigma_j}$, which can be calculated as

$$\Gamma_{\varsigma_i,\varsigma_j} = \max \quad \left(\varsigma_i, \varsigma_j\right) + \left(1 - \lambda_{i,j}\right) \min\left(\varsigma_i, \varsigma_j\right), \tag{1}$$

where $\lambda_{i,j}$ is the correlation coefficient of ς_i and ς_j and $\lambda_{i,j}$ can be calculated as

$$\lambda_{i,j} = \frac{1}{e^{(d_{i,j}^2/\beta)}}. \tag{2}$$

$d_{i,j}$ is the distance between ς_i and ς_j and β is the constant of correlation coefficient, while $\beta \to 0$ and $\lambda_{i,j} \to 0$, indicating there is no correlation between ς_i and ς_j, and the larger β is, the higher data correlation of them is.

3.2. Network Parameters. A sensor node is composed of a sensing unit and a communication unit [17], the sensing unit is responsible for sensing the monitoring event and invoking the communication unit after sensing the event, and then the communication unit initiates its internal communication mechanism to transmit data to the sink. Due to the fact that the energy of nodes is strictly limited, the sensor nodes use sleep/waking cycling mode to save energy [15]. In one unit cycle, the nodes are in the sleeping and waking state periodically, and only when the node is in the waking state can it perceive events and transmit data. In one unit cycle, the ratio of the node in the waking state to the whole cycle is called duty cycle; suppose that ϕ_S is the sensing duty cycle and ϕ_C is the communication duty cycle, and then

$$\begin{aligned} \phi_S &= \frac{\mathcal{T}_S^a}{\mathcal{T}_S^s + \mathcal{T}_S^a} = \frac{\mathcal{T}_S^a}{\mathcal{T}_{\text{SEN}}} \\ \phi_C &= \frac{\mathcal{T}_C^a}{\mathcal{T}_C^s + \mathcal{T}_C^a} = \frac{\mathcal{T}_C^a}{\mathcal{T}_{\text{COM}}}, \end{aligned} \tag{3}$$

where $\mathcal{T}_{\text{SEN}}$ is the sensing cycle, $\mathcal{T}_{\text{COM}}$ is the communication cycle, $\mathcal{T}_S^a$ is the time that the node is in the waking state during the sensing cycle, $\mathcal{T}_S^s$ is the time that the node is in the sleeping state during the sensing cycle, $\mathcal{T}_C^a$ is the time that the node is in the waking state during the communication cycle, and $\mathcal{T}_C^s$ is the time that the node is in the sleeping state during the communication cycle.

The energy consumption model of this paper is similar to [14, 41], and the energy consumption of nodes is composed of event sensing, data transmission, data receiving, and low power listening. Therefore, the energy consumption model can be expressed as

$$E_{\varsigma_i} = €_{\text{Se}}^i + €_{\text{Td}}^i + €_{\text{Rd}}^i + €_{\text{Lp}}^i. \tag{4}$$

Table 1: Network parameters.

Parameter	Value	Description
$\overline{E}_{\text{Ini}}$	0.5	Initial energy (J)
$\mathcal{T}_{\text{SEN}}$	15	Sensing cycle (s)
$\mathcal{T}_{\text{COM}}$	100	Communication cycle (ms)
d_{Pr}	0.26	Preamble duration (ms)
d_{Ac}	0.26	Acknowledge window duration (ms)
d_{Da}	0.93	Data packet duration (ms)
$\mathcal{E}_T$	0.0511	Power consumption in transmission (w)
$\mathcal{E}_R$	0.0588	Power consumption in receiving (w)
$\mathcal{E}_{\text{Se}}$	0.0036	Power consumption in sensing (w)
$\mathcal{E}_{\text{Sl}}$	$2.4 * 10^{-7}$	Power consumption in sleeping (w)

Table 1 and the Parameters Related to Calculation list the relevant parameters used in this paper, and the parameters values are derived from the internal data tables of the prototype sensor nodes as in [7].

3.3. Problem Statements. The main objective of this paper is to design an efficient communication scheme suitable for wireless sensor networks. In the quality of service, the scheme can meet different delay requirements. In terms of network performance, the scheme is able to maintain the network lifetime while strengthening the effective use of energy. It can be expressed as follows.

(1) Minimize End-to-End Delay for Delay-Sensitive Data. The end-to-end transmission delay of data refers to the time required from the preparation of data at the sender to its arrival at the sink [17, 42]. Assuming that the transmission delay of kth hop is d_{h_k}, and the number of relay hops is $\mathcal{N}$, then the minimized end-to-end delay is expressed as follows:

$$\min \quad (D_{e2e}) = \min\left(\sum_{1\le k\le \mathcal{N}} \mathrm{d}_{h_k}\right). \tag{5}$$

(2) Balance Energy Consumption and Maximize Energy Utilization. All data in the network are transmitted to the sink via multihop relays. This sink-centered data gathering model results in a large amount of data and energy consumption in the area that is relatively close to the sink [11, 43, 44], while, in the area far away from the sink, the energy consumption is very small, which contributed to an imbalance in the energy consumption. Assuming that there are N nodes in the network, the energy consumption of node ς_i is E_{ς_i}, and the equilibrium energy consumption of the network is to minimize the energy difference between the maximum energy consumption and the minimum energy consumption; that is,

$$\min \quad (E_{\text{dif}}) = \min\left(\max_{1\le i\le N}\left(E_{\varsigma_i}\right) - \min_{1\le j\le N}\left(E_{\varsigma_j}\right)\right). \tag{6}$$

Energy utilization is the ratio of the energy consumed by the network to the initial energy. Assuming that the initial energy of the node ς_i is $\overline{E}^i_{\text{Ini}}$, the maximized energy utilization can be expressed as follows:

$$\max \quad (\mathcal{R}_{e\_\text{uti}}) = \max\left[\frac{\left(\sum_{1\le i\le N} E_{\varsigma_i}\right)}{\left(\sum_{1\le i\le N} \overline{E}^i_{\text{Ini}}\right)}\right]. \tag{7}$$

(3) Maximize Network Lifetime. Network lifetime is the data transmission rounds that have been performed before the death of the network, which is defined in most studies as the death time of the first node in the network [12, 45, 46]. In wireless sensor networks, the node is powered by the battery, and when the energy of the node is exhausted, the node dies [47]. Therefore, the network lifetime depends on the maximum energy consumption of the network. Assuming that the energy consumption of the node ς_i is E_{ς_i}, its initial energy is $\overline{E}_{\text{Ini}}$, and there are N nodes in the network. Therefore, the maximized lifetime of the network is to maximize the lifetime of the node with the largest energy consumption; that is,

$$\max \quad (\mathcal{F}_\ell) = \max\left[\frac{\overline{E}_{\text{Ini}}}{\max_{1\le i\le N}\left(E_{\varsigma_i}\right)}\right]. \tag{8}$$

In summary, the research objectives are as follows:

$$\begin{aligned}
&\min \quad (D_{e2e}) = \min\left(\sum_{1\le k\le \mathcal{N}} \mathrm{d}_{h_k}\right)\\
&\min \quad (E_{\text{dif}}) = \min\left(\max_{1\le i\le N}\left(E_{\varsigma_i}\right) - \min_{1\le j\le N}\left(E_{\varsigma_j}\right)\right)\\
&\max \quad (\mathcal{R}_{e_\text{uti}}) = \max\left[\frac{\left(\sum_{1\le i\le N} E_{\varsigma_i}\right)}{\left(\sum_{1\le i\le N} \overline{E}^i_{\text{Ini}}\right)}\right]\\
&\max \quad (\mathcal{F}_\ell) = \max\left[\frac{\overline{E}_{\text{Ini}}}{\max_{1\le i\le N}\left(E_{\varsigma_i}\right)}\right].
\end{aligned} \tag{9}$$

4. DSDR Scheme

4.1. Research Motivation. Applications running on the same network platform may have different latency requirements

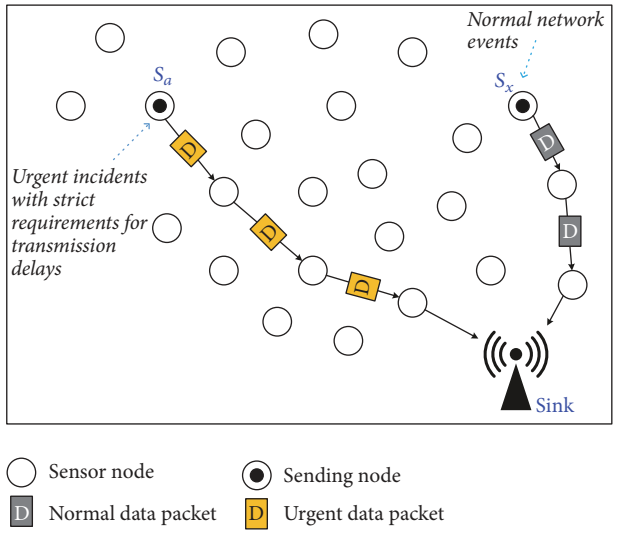

Figure 1: Traditional data routing for different events.

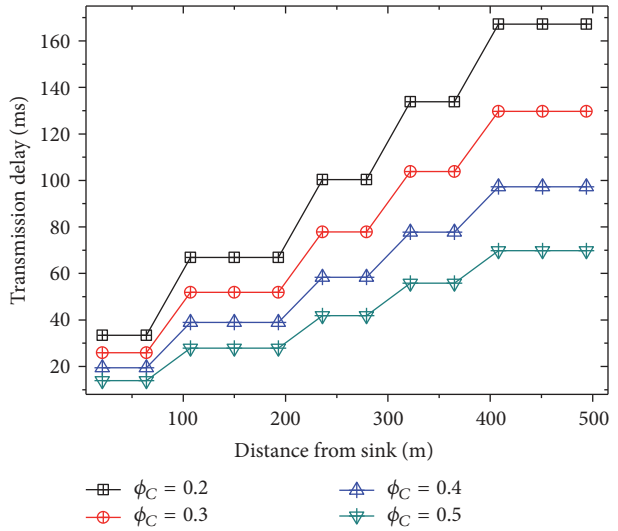

Figure 2: Transmission delay for different distances from the sink.

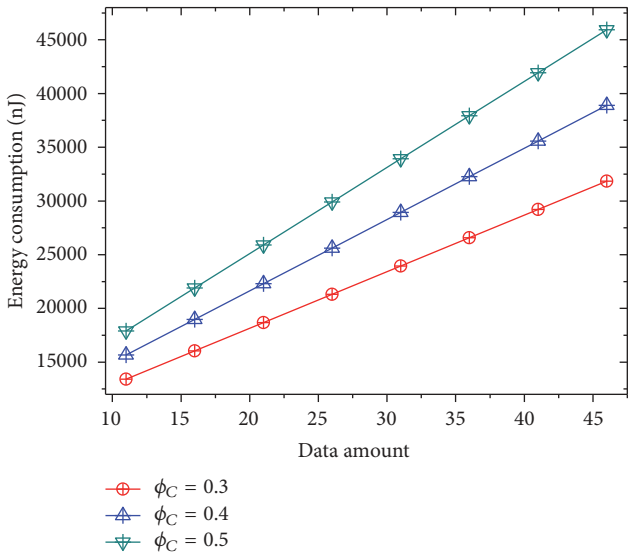

Figure 3: Energy consumption for different data amount.

due to the differences in events [3, 48], and most existing schemes cannot intelligently select appropriate data routing based on the latency sensitivity of the events, thus failing to meet the requirements of different data. For example, in a network applied to biological monitoring, the sensor nodes are usually deployed to record the daily behaviors of the organism, but if the organism gets into danger and its vital signs change dramatically, it is required to transfer the urgent data to decision-makers as soon as possible in order to take corresponding rescue measures in time. Therefore, for such networks, the difference of its service quality is embodied in the following: for delay-sensitive data, it is required to transmit information to the sink as soon as possible through a reliable transmission mechanism, and for delay-tolerant data only the normal transmission is required. As shown in Figure 1, ς_a and ς_x are two nodes in the network, where ς_x senses normal events that carry delay-tolerant data, while ς_a senses urgent incidents which have strict requirements for the transmission delay. According to the urgency of the packets, the data sent by ς_a should be transmitted to the sink earlier than ς_x. But, in the wireless sensor networks, the packets are relayed to the sink through multi hops, and the maximum forwarding distance at each hop for nodes is r, where r is the communication radius of nodes. Therefore, the farther the distance between the sending node and the sink is, the more relay hops the data passes, and the greater the transmission delay is, so, in the previous studies, the data of ς_a in Figure 1 is much more delayed than that of ς_x, which conflicts with the latency requirements of the data.

In a sparse network with $R = 500$, $r = 80$, and $\rho = 0.1$, suppose nodes adopt 0-1 communication mode and data transmission adopts multihop routing; then the network performance under different parameter values is shown in Figures 2–6. When the node communication duty cycle is 0.2–0.5, respectively, the end-to-end delay at different distances of the network is shown in Figure 2. It can be seen from Figure 2 that the transmission delay of data gradually increases with the distance from the sink, and the delay of the far-sink region is much higher than that of the near-sink region, which is about 4 times ($\phi_C = 0.2$). And the near-sink region refers to the region within one-hop range of the sink, in a network where the network radius is 500 and the node communication radius is 80, the area whose distance from the sink is 0–80 is near-sink region, and nodes located in the near-sink area are near-sink nodes. Similarly, the far-sink region refers to the area outside one-hop range of the sink, which is an area whose distance from the sink is 80–500, and the nodes in this area are far-sink nodes. It is clear that the far-sink area occupies a large area of the network, so the probability that the delay-sensitive events are distributed in the far-sink area is much higher than that of the near-sink area, and this raises the requirements for the service quality of the network, especially the transmission delay in

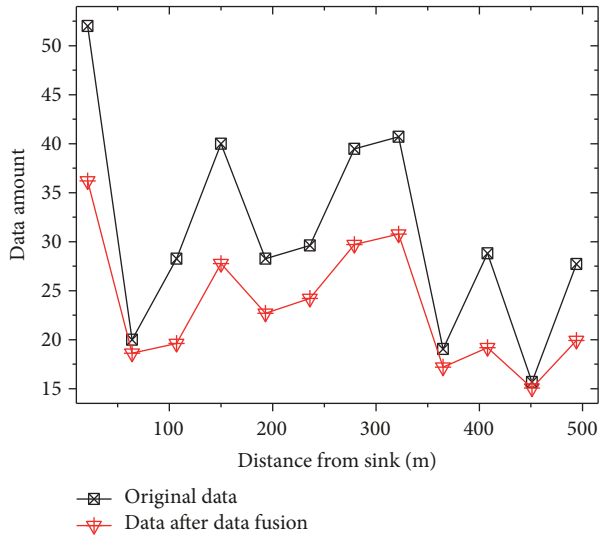

Figure 4: Data amount before and after data fusion.

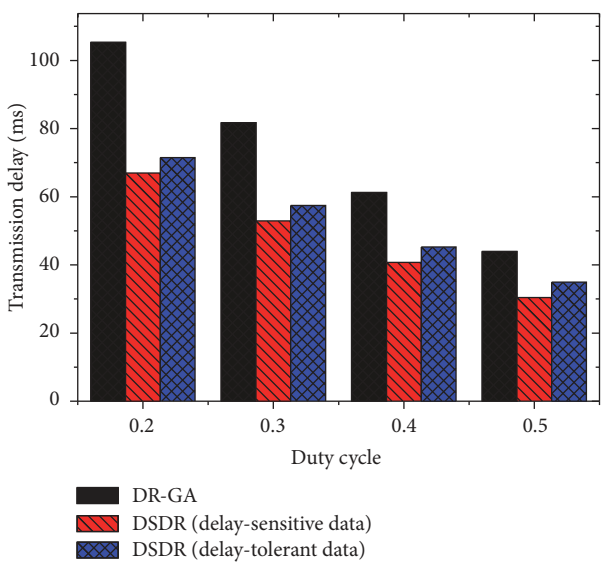

Figure 5: Transmission delay in DR-GA and DSDR.

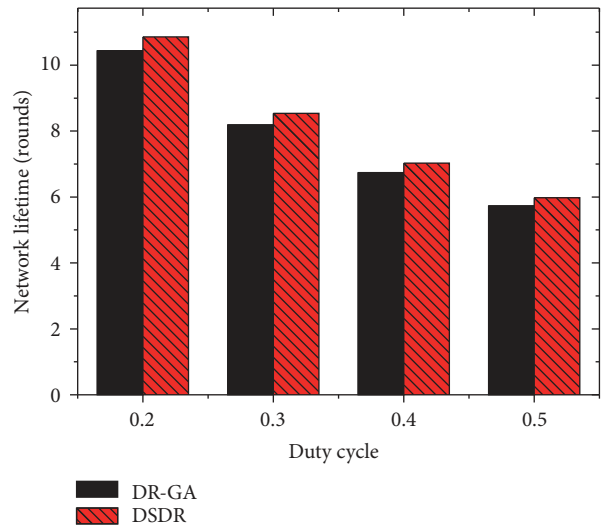

Figure 6: Network lifetime in DR-GA and DSDR.

the far-sink area. In addition, to overcome the limited energy of the nodes and the difficult replacement of batteries, the sleep/waking working mode is used to save energy [15], and the node can forward data only when it is in the waking state. Obviously, prolonging the time of the node in the waking state can effectively reduce the waiting delay, thus improving the transmission efficiency.

This can also be seen from Figure 2, compared with the lower duty cycle 0.2, when the duty cycle is 0.5, the network delay is greatly reduced, and the maximum delay in far-sink area is shortened from 167.25 ms to 69.75 ms.

Increasing the duty cycle can effectively reduce the transmission delay, but this is at the expense of energy consumption. Because the energy consumption of nodes in the waking state is 100–1000 times that in the sleeping state [5, 12, 23], therefore, if the duty cycle of all nodes in the network increases, it will greatly exacerbate the network energy consumption and shorten the network lifetime. According to the energy consumption model of (4), the energy consumption of nodes is caused by event sensing, data transmission, data receiving, and low power listening, where energy consumption in sensing and low power listening are related to the node's sensing and communication cycle, and the cycles are constant. The energy consumption in data transmission and receiving are affected by data amount. When the node communication duty cycle is 0.3, 0.4, and 0.5, respectively, the energy consumption of the network under different data amount is given in Figure 3. As shown in Figure 3, the energy consumption increases linearly as the amount of data increases, and the larger the data amount is, the more energy it consumes, and, at the same time, the larger the duty cycle is, the faster the energy consumption increases.

It can be seen from Figure 3 that reducing the amount of data is the key to saving energy. Numerous studies have shown that network data are correlated with each other in time and space, and there is redundancy among the data detected by multiple nodes of the event [3, 22]. Therefore, data fusion technology can be used to aggregate the information of multiple events and then send it to the sink, thus greatly reducing the amount of data and energy consumption. When the probability of generating data is 0.1, the data fusion rate is between 0.1 and 0.3, and the comparison of data amount before and after data fusion is shown in Figure 4. Since the fusion rate between any two data packets is random and uncertain, the amount of data after fusion for different data varies. However, in general, compared with the original data, the data amount is greatly reduced after fusion.

As mentioned in Figure 4, improving the node duty cycle can effectively reduce delay, while using data fusion can alleviate the energy consumption caused by the increase of duty cycle. However, from the perspective of data generation, in general, the data transmitted in the network are delay-tolerant data; that is, the probability of generating delay-sensitive data is relatively small, and for these small

probability data improving duty cycles of all nodes, obviously, is not the most reasonable solution. Therefore, it can only increase the duty cycles of a small part of nodes and establish energy-efficient routing paths by these nodes and finally relay the delay-sensitive data to the sink via these paths; as for delay-tolerant data, data fusion is performed at each hop on the path to save energy, and we called this communication scheme DSDR (delay Differentiated Services for Data Routing).

In the same network scenario as Figure 2, if the DSDR scheme is adopted, then the comparison between DSDR scheme and DR-GA scheme in terms of latency and network lifetime is given in Figures 5 and 6, where the DR-GA (General Data Routing Approach) represents the routing scheme widely used in other studies, the data transmission under this scheme also uses multihop relaying, and the relay node selection is based on the shortest distance. As can be seen from Figure 5, compared with the DR-GA scheme, the transmission delay under the DSDR scheme is greatly reduced, and the latency of delay-sensitive data is smaller than that of delay-tolerant data, which means that DSDR can provide differentiated services while ensuring low transmission latency. More importantly, although the DSDR scheme can effectively reduce the network delay, as shown in Figure 6 it has a longer network lifetime than the DR-GA scheme, which also shows the advantage of the DSDR scheme.

4.2. General Design of DSDR. The main idea of DSDR is to establish energy-efficient routing paths (E2RPs) at different locations of the network, and the communication duty cycles of nodes on E2RPs are increased to 1 (except for the nodes in the near-sink area), and then transmit data to the sink through these E2RPs by adopting different routing methods for different data.

In general, the data communication under DSDR includes the following phases.

Phase 1 (establishment of energy-efficient routing paths (E2RPs)). Each node in the network is required to store two values: $\mathcal{Q}_{tS}$ and $\mathcal{Q}_{tR}$, where $\mathcal{Q}_{tS}$ is the minimum hops to the sink and $\mathcal{Q}_{tR}$ is the minimum hops to E2RPs. Before the establishment of E2RPs, the values of $\mathcal{Q}_{tS}$ and $\mathcal{Q}_{tR}$ are *POSITIVE_INFINITY*, and the values of them are constantly updated with the constant broadcast in the network. The general process is as follows: firstly, starting from the sink, it broadcasts the latest $\mathcal{Q}_{tS}$ to the nodes in the communication range, which is valued 1, and then the nodes that receive the broadcast message compare $\mathcal{Q}_{tS}$ in the broadcast with its stored value and update its $\mathcal{Q}_{tS}$ to the smaller value and then repeat the same process, and then each node determines its $\mathcal{Q}_{tS}$ by continuous diffusion of broadcasting. Then, starting from a node in the network, for each hop, select a node whose $\mathcal{Q}_{tS}$ is smaller than its own in the communication range to establish a path to the sink (i.e., an E2RP), and then configure the duty cycle and $\mathcal{Q}_{tR}$ of the nodes on this E2RP. Finally, $\mathcal{Q}_{tR}$ of each node is determined by the same broadcast diffusion as $\mathcal{Q}_{tS}$ in the center of each node on the E2RP. In a similar way, a number of E2RPs in other areas are established.

Phase 2 (delay differentiated services for different data). After E2RPs are established, all the data is transferred to the sink through E2RPs, and different transmission methods are adopted according to different delay requirements of the data. First, for the delay-sensitive data, a direct-forwarding routing method is adopted, the specific process is as follows: starting from the sending node, each time the node selects a node whose $\mathcal{Q}_{tR}$ is smaller than its own in the communication range as the next-hop node. This process continues until $\mathcal{Q}_{tR}$ of the next node becomes 0, which means that the data has reached the nearest E2RP and then use the E2RP to transmit data to the sink. During the entire transmission process, the data is not stopped. Then, for delay-tolerant data, a waiting-forwarding routing method is adopted, and its data routing process is the same as delay-sensitive data, which is also transmitted to the sink through the nearest E2RP and under the guidance of $\mathcal{Q}_{tR}$, but delay-tolerant data stays for a certain amount of time at each hop for maximum data fusion, and the specific dwell time is determined by the delay requirements of the data.

Phase 3 (data fusion for delay-tolerant data). Starting from the sending node, data fusion is performed at each relay hop. Firstly, the maximum waiting time at each hop is obtained according to the total waiting time of the data and the distance from the sending node to the sink and the E2RP. Then, the data stops for corresponding time at each relay to merge with other packets received by the relay. After the waiting duration is reached, the fused data are transmitted to the next hop. And the above process is repeated until the data are transferred to the sink.

Figure 7 is the data routings for different data in DSDR. The data routing of delay-tolerant data and delay-sensitive data is described with an E2RP as an example. Compared to delay-tolerant data, delay-sensitive data has a higher transmission priority. When the delay-sensitive data are perceived, the sensing node immediately transmitted it to the sink via E2RP, and there is no stop during the transmission. And for delay-tolerant data, such as data in Area 1 and Area 2, after the node senses the data, it is transmitted to the next hop, and then the next hop node waits for more packets around it to arrive. When the corresponding waiting time for the data is up, the relay node merges all the data it receives with the packet to remove the redundant information and then forwards it to the next hop. As we can see, the delay-tolerant data is fused at each hop it passes.

4.3. Implementation of DSDR. In DSDR, each E2RP forwards events in its vicinity; therefore, the transmission quality of the path directly affects the performance of the entire network. In addition, the amount of data carried by the E2RP is very large, and the nodes on the path are awake all the time; therefore, the energy consumption of E2RPs is very serious, so the establishment and switching of the E2RPs are an important issue. On the other hand, how to determine the urgency of data, define its data type, and set the maximum waiting time at each hop is essential for data routing. And, for the delay-tolerant data in the network, the specific calculation of data

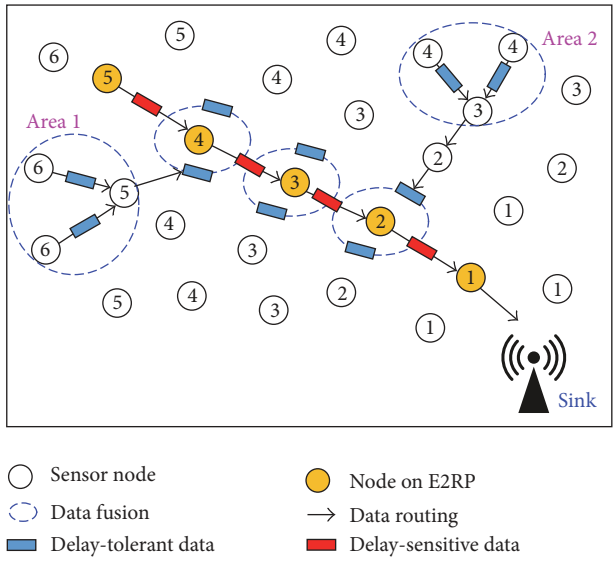

Figure 7: Different data routing for data in DSDR.

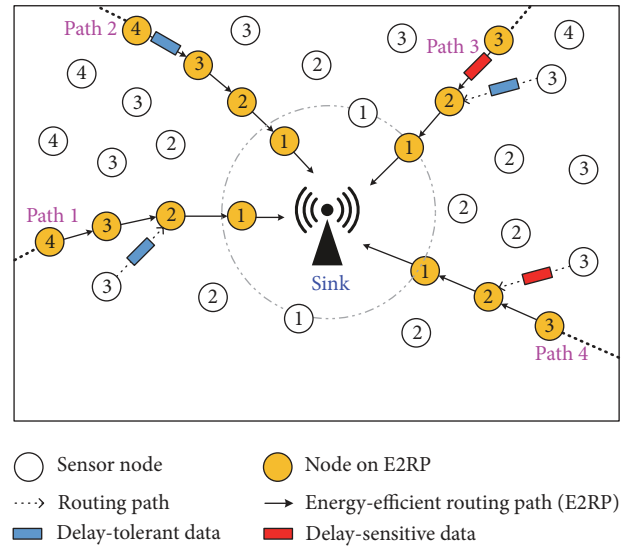

Figure 8: Energy-efficient routing paths in DSDR.

fusion is also an important issue, and we mainly discuss the implementation of these in this section.

(1) Establishment and Switching of E2RP. Not every node that generates a packet will establish an E2RP, and the establishment of E2RPs only happens in two phases: (a) network initialization and (b) when an E2RP is removed. The specific establishment of an E2RP is divided into three scenarios: (1) *Confirmation of Minimum Hops to the Sink*. The confirmation of $\mathcal{Q}_{tS}$ is based on the acquisitions of neighbors' information by broadcast diffusion; when the network is initialized, the sink sets its $\mathcal{Q}_{tS}$ to 0, and the other nodes set their $\mathcal{Q}_{tS}$ to ∞. Then, the sink sends a broadcast message to nodes in its communication range, informing them of the latest $\mathcal{Q}_{tS}$, which is $sink.\mathcal{Q}_{tS} + 1$. Each node that received the broadcast information compares the broadcast value with its stored $\mathcal{Q}_{tS}$. If the value is smaller than the previously stored $\mathcal{Q}_{tS}$, $\mathcal{Q}_{tS}$ of the node is reassigned to the broadcast value. Then, the node that has updated $\mathcal{Q}_{tS}$ broadcasts the latest $\mathcal{Q}_{tS}$ to other nodes, which is $\mathcal{Q}_{tS}$ of this node plus 1. The whole process continues until all nodes in the network are not continually updated to ensure that each node confirms its $\mathcal{Q}_{tS}$. (2) *Establishment of an E2RP*. After each node in the network has confirmed its $\mathcal{Q}_{tS}$, starting from the sending node, for each hop, select a next hop whose $\mathcal{Q}_{tS}$ is smaller than its own from the neighboring nodes in the communication range. This process continues until $\mathcal{Q}_{tS}$ of the relay node becomes 0, which means that the data has reached sink. Then $\mathcal{Q}_{tR}$ of all relay nodes on the path are set to 0 and the communication duty cycles of these nodes are set to 1, except for nodes in near-sink region. (3) *Confirmation of the Minimum Hops to E2RPs*. Making each node on the E2RPs as the center, determine $\mathcal{Q}_{tR}$ of each node by the same broadcast diffusion of $\mathcal{Q}_{tS}$. In a similar way, a number of E2RPs in other areas are established.

As shown in Figure 8, there are four E2RPs in the network: Paths 1–4. $\mathcal{Q}_{tS}$ of each node in the figure is centered on the sink and incremented from inside to outside. $\mathcal{Q}_{tR}$ of the node is not marked in this figure, but it can be seen from the data routing of nodes, whether delay-tolerant data or delay-sensitive data, once the sending node senses the data, the node will transmit it through the nearest E2RP, and, in fact, it is completed under the guidance of $\mathcal{Q}_{tR}$. Assuming that $\mathcal{Q}_{tS}$ in each broadcast message is $\mathcal{Q}^*_{tS}$, $\mathcal{Q}_{tR}$ in each broadcast message is $\mathcal{Q}^*_{tR}$, the communication duty cycle is ϕ_C, and the *Nodes.br* is used to identify whether nodes have received or sent broadcast messages before, and then the establishment and configuration of an E2RP are described by Algorithm 1.

The energy consumption of the E2RPs is serious. Because the lifetime of network is determined by the maximum energy consumption of nodes, in order to avoid the energy consumption of E2RPs shortening the network lifetime, we measure the residual energy of the E2RPs periodically and switch it at appropriate time. The principle of switching and reconstructing the E2RPs is as follows: for each E2RP in the network, the residual energy of its nodes is measured at intervals of time, and once the energy is lower than the threshold, which is set to 20%–30% of the initial energy, the path is immediately removed and the parameters of nodes on it are restored to the system initial values, and all nodes on the path no longer act as E2RPs nodes. Then find new relay nodes which are located in the far-sink area and have a large amount of residual energy. And the establishment of the new E2RP is similar to Scenario 2 in Algorithm 1, but the remaining energy is taken into account when selecting relay nodes on E2RPs. If the residual energy of the node is below the threshold, then it will not serve as a relay node on E2RPs.

(2) Setting of Data Urgency and Waiting Time. There are two types of data under the DSDR scheme, one is delay-sensitive data, which is denoted as $\mathbb{D}_{ds}$, and the other is delay-tolerant data, which is denoted as $\mathbb{D}_{or}$. Each packet has a parameter φ^e to identify the urgency of its data; when φ^e is true, it means that the data are delay-sensitive data; and when φ^e

(1) Initialize: *Sink*. $\mathcal{Q}_{tS} = 0$, *Nodes*. $\mathcal{Q}_{tS} = \infty$, *Nodes*. $\mathcal{Q}_{tR} = \infty$, $Nodes._{br} = false$
(2) **Scenario 1**: *Determining the* $\mathcal{Q}_{tS}$ *of each node*
(3) Let $\varsigma_{\text{bro}} = Sink$
(4) **Loop 1**: ς_{bro} broadcasts $\mathcal{Q}^*_{tS}$ in its communication range, where $\mathcal{Q}^*_{tS} = \varsigma_{\text{bro}}.\mathcal{Q}_{tS} + 1$
(5) **For** each ς_i in communication range **and** $\varsigma_{i\cdot br} = false$ **Do**
(6) ς_i receives the broadcast message
(7) **If** $\varsigma_{i.}\mathcal{Q}_{tS} > \mathcal{Q}^*_{tS}$ **then**
(8) $\varsigma_{i.}\mathcal{Q}_{tS} = \mathcal{Q}^*_{tS}$
(9) $\varsigma_{i\cdot br} = true$
(10) $\varsigma_{\text{bro}} = \varsigma_i$
(11) **Goto Loop 1**
(12) **End if**
(13) **End for**
(14) **Scenario 2**: *Establishment of an E2RP*
(15) Let ς_j as the first node on the path
(16) Let $\varsigma_{\text{next}}.\mathcal{Q}_{tS} = \varsigma_j.\mathcal{Q}_{tS}$
(17) **While** $\varsigma_{\text{next}}.\mathcal{Q}_{tS} > 0$ **Do**
(18) Find ς_k in communication range: $\varsigma_k.\mathcal{Q}_{tS} < \varsigma_{next}.\mathcal{Q}_{tS}$
(19) Let $\varsigma_{\text{next}} = \varsigma_k$
(20) **End while**
(21) Let $\mathcal{Q}_{tR}$ of all nodes on the path to 0
(22) Let ϕ_C of far-sink nodes on the path to 1
(23) **Scenario 3**: *Determining the* $\mathcal{Q}_{tR}$ *of each node*
(24) **For** each ς_n on the E2RP **Do**
(25) Let$\varsigma_{\text{bro}} = \varsigma_n$
(26) **Loop 2:** ς_{bro} broadcasts $\mathcal{Q}^*_{tR}$ in its communication range, where $\mathcal{Q}^*_{tR} = \varsigma_{\text{bro}}.\mathcal{Q}_{tR} + 1$
(27) **For** each ς_i in communication range of ς_{bro} **Do**
(28) ς_i receives the broadcast message
(29) **If** $\varsigma_{i.}\mathcal{Q}_{tR} > \mathcal{Q}^*_{tR}$ **then**
(30) $\varsigma_{i.}\mathcal{Q}_{tR} = \mathcal{Q}^*_{tR}$
(31) $\varsigma_{\text{bro}} = \varsigma_i$
(32) **Goto Loop 2**
(33) **End if**
(34) **End for**
(35) **End for**

Algorithm 1: Establishment of energy-efficient routing path.

is false, it represents delay-tolerant data. The waiting time for delay-sensitive data is 0 and for delay-tolerant data is W_T, and the value of W_T varies with the specific situation of data. Depending on W_T of data and the distance between the sensing node and the sink, the waiting duration at each hop is determined, as shown in Theorem 1.

Theorem 1. *Suppose that* $\mathbb{D}^i_{or}$ *is a delay-tolerant data packet whose distance from sink is i, the waiting time of* $\mathbb{D}^i_{or}$ *is* W^i_T*, its hops to E2RP are* $\mathcal{Q}^i_{tR}$*, and the hops from E2RP to the sink are* $\mathcal{Q}^i_{R2S}$*, and then the waiting duration at each hop for* $\mathbb{D}^i_{or}$ *can be expressed as follows:*

$$T^{\mathbb{D}^i_{or}}_{one} = \frac{W^i_T}{\mathcal{Q}^i_{tR} + \mathcal{Q}^i_{R2S}} - \Delta\tau. \tag{10}$$

Proof. The total waiting time of $\mathbb{D}^i_{\text{or}}$ is W^i_T, and the transmission from the sensing node to the sink is composed of two phases: one is the data transmission from the sensing node to the E2RP, and the number of relay hops in this phase is $\mathcal{Q}^i_{tR}$; the other is the transmission from the E2RP to the sink, and the number of relay hops in this phase is $\mathcal{Q}^i_{R2S}$. Therefore, the total number of relay hops from the sensing node to the sink is $\mathcal{Q}^i_{tR} + \mathcal{Q}^i_{R2S}$. Then the waiting duration at each hop is obtained by dividing the total waiting time by total relay hops, that is, $W^i_T/(\mathcal{Q}^i_{tR} + \mathcal{Q}^i_{R2S})$. However, it should be noted that since W^i_T is the maximum waiting time of the data and there are some other delays in the transmission, therefore, the actual waiting duration at each hop is $W^i_T/(\mathcal{Q}^i_{tR} + \mathcal{Q}^i_{R2S}) - \Delta\tau$, where $\Delta\tau$ is the other delays that may be encountered

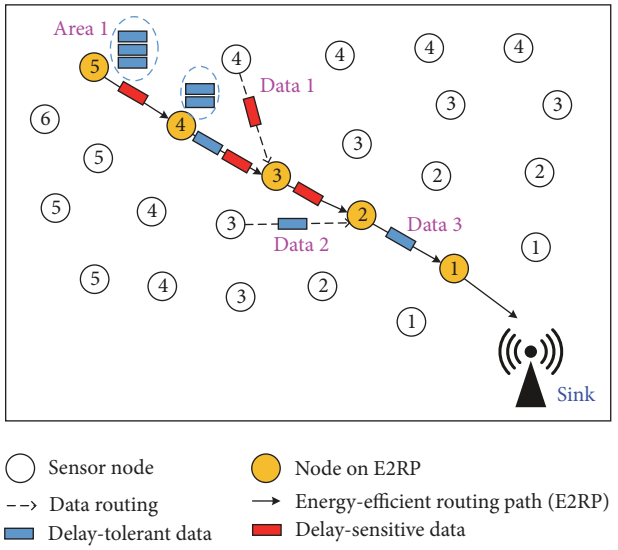

FIGURE 9: Data routing and waiting time for different data.

on the transmission path, including queuing and possible retransmission delays. In a sparse network with good link quality, $\Delta\tau$ can be ignored. □

After the data type and one-hop waiting duration are confirmed, the data can be routed as in Figure 9. The waiting time of delay-sensitive data in the network is 0, and once the data are sensed, they are quickly transmitted to the sink via E2RP, such as Data 1 and other delay-sensitive packets on E2RP in the figure. When delay-tolerant data are sensed, they are waiting for $T_{\text{one}}^{\mathbb{D}_{\text{or}}^{i}}$ time at each hop to fuse with other data received by the relay, such as Data 2 in the figure. Three delay-tolerant packets in Area 1 are waiting to be merged with other data because of their one-hop waiting time, while the waiting time for Data 3 is reached and it is forwarded to the next hop through E2RP.

(3) Related Implementation of Data Fusion. Data fusion rules of the delay-tolerant data are as follows: data stay $T_{\text{one}}^{\mathbb{D}_{\text{or}}^{i}}$ time at each hop of the data routing. In $T_{\text{one}}^{\mathbb{D}_{\text{or}}^{i}}$, the data wait for the other packets received by the relay node to fuse, and once $T_{\text{one}}^{\mathbb{D}_{\text{or}}^{i}}$ time is reached, the merged data are sent to the next hop.

In this paper, the nodes have different data amount due to the different positions, and the trend of data amount is as follows: (A) the closer the node is to the sink, the larger its data amount is, the data amount of the nodes in the near-sink area is large, and that of far-sink area is small. (B) The closer the node is to the E2RP, the larger its data amount is, and the data amount of nodes that are far away from the E2RP and the sink is small.

According to [14], suppose that the network radius is R, the node communication radius is r, the probability of generating data is P_d, ς_d^i is the node whose distance to the sink is i, and Z is the largest positive integer that makes the expression $i + Zr < R$ true, and then the number of packets received by ς_d^i can be expressed as follows:

$$\Pi_R^i = \left[(Z+1) + \frac{Z(Z+1)r}{2i}\right] P_d \quad \text{where } i + Zr < R. \tag{11}$$

Theorem 2. *In DSDR, suppose that the network radius is R, the node communication radius is r, the probability of generating data is P_d, ς_d^i is the node whose distance to the sink is i, the distance from ς_d^i to its nearest E2RP is K_e^i, and then the number of packets received by ς_d^i in this paper can be expressed as follows:*

$$\Pi_{Rec}^i = \max\left(\left[(Z+1) + \frac{Z(Z+1)r}{2i}\right] P_d, \left[(Z+1) + \frac{Z(Z+1)r}{2\mathrm{K}_e^i}\right] P_d\right) \quad \textit{where } i + Zr < R. \tag{12}$$

Proof. Equation (11) gives the data packets of nodes in a network with the sink as the center: $[(Z+1) + Z(Z+1)r/2i]P_d$, where Z is the largest positive integer that makes the expression $i + Zr < R$ true. In this paper, the data of the far-sink region are all transmitted through the E2RPs, so the data packets of the far-sink nodes in the network decrease gradually with the distance from the E2RP. When the distance from ς_d^i to its nearest E2RP is K_e^i, according to [14], the data packets of nodes in a network with E2RPs as the center are $[(Z+1) + Z(Z+1)r/2\mathrm{K}_e^i]P_d$. However, the regions in the network are overlapped, and the data packets in regions closer to the sink are much larger when it is centered on the sink than centered on E2RPs and vice versa, so the data packets actually assumed by the nodes in the network should be the larger of the two cases, which is (12). □

In DSDR, the data fusion is performed after each relay node located on the transmission path receives a delay-tolerant packet. Suppose that the number of delay-tolerant packets received by ς_M is $\Pi_{\text{Rec}}^{\varsigma_M}$, the packet length is δ_o, and $\mathscr{E}_\lambda = 1 - \lambda_\vartheta$, where λ_ϑ is the correlation coefficient of data, and, according to (1) and [24], the amount of data received by ς_M can be expressed as follows:

$$\varphi_{\text{Rec\_1}}^{\varsigma_M} = \mathscr{E}_\lambda \Pi_{\text{Rec}}^{\varsigma_M} \delta_o + \delta_o = \delta_o \left(\mathscr{E}_\lambda \Pi_{\text{Rec}}^{\varsigma_M} + 1\right). \tag{13}$$

According to (13), suppose that the number of delay-tolerant packets is Π_{dt}, the packet length is δ_o, and $\mathscr{E}_\lambda = 1 - \lambda_\vartheta$, where λ_ϑ is the correlation coefficient of data, and then the amount of data after fusing k times can be expressed as follows:

$$\varphi_k = \left(\mathscr{E}_\lambda\right)^k \Pi_{dt} \delta_o + \delta_o = \delta_o \left[\left(\mathscr{E}_\lambda\right)^k \Pi_{dt} + 1\right]. \tag{14}$$

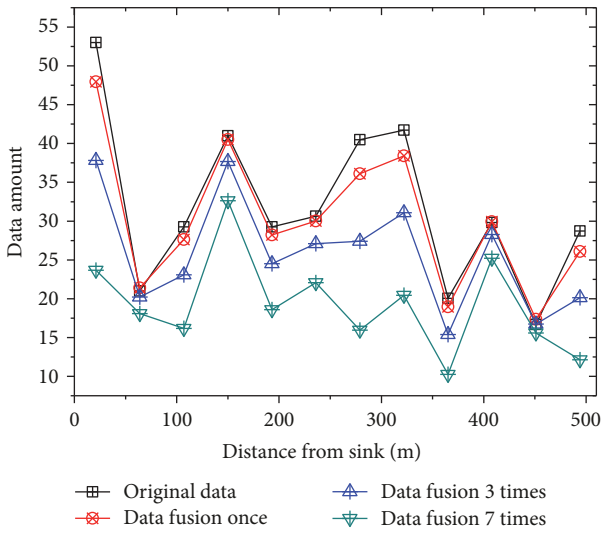

Figure 10: Data amount for different data fusion times.

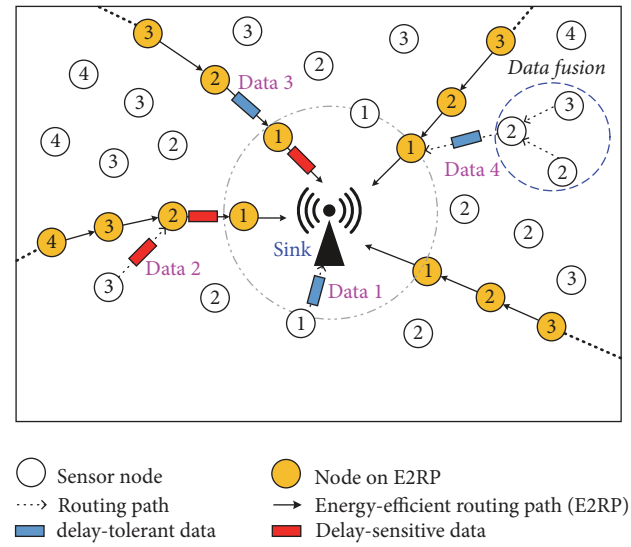

Figure 11: Data routing in DSDR.

In a circular network with a radius of 500 and a node communication radius of 100, a data fusion rate of 0.01–0.15, the data amount of the network under different fusion times is given in Figure 10. It can be seen from the figure that data fusion can effectively reduce data amount, but, because of the uncertainty of the data correlation of packets in the network, the data fusion rate between packets is also different. Generally, data relevance for the packets sensed at the same time and space is higher. Observing the circumstances under different data fusion times, it is found that the data amount decreases with the increase of the fusion times. Since the data redundancy becomes less and less in the process of continuous fusion, when the number of fusions reaches a certain level, the reduction in the amount of data is less obvious.

After the E2RPs are established and the data fusion rules are confirmed and the routing rules are shown in Figure 11, consider the following.

(1) For data in the near-sink area, they are sent directly to the sink regardless of the data type, as Data 1 in Figure 11.

(2) For delay-sensitive data in far-sink area, they are transmitted to the sink via the E2RP, as Data 2 in Figure 11.

(3) For the delay-tolerant data in the far-sink area, they are also transmitted to the sink through the E2RP, but the $T_{\text{one}}^{\mathbb{D}_{\text{or}}^i}$ time is reserved at each hop to fuse with other data received by the node. After the waiting time is reached, the merged data are transferred to the next hop, as Data 3 and Data 4 in Figure 11.

Suppose that the node that senses the data is ς_{tr}, the relay hops from ς_{tr} to the sink are $\varsigma_{tr}.\mathcal{Q}_{tS}$, and the relay hops from ς_{tr} to E2RP are $\varsigma_{tr}.\mathcal{Q}_{tR}$; if the data are delay-tolerant data, φ^e is false, if the data are delay-sensitive data, φ^e is true, and the waiting duration for delay-tolerant data at each hop is $T_{\text{one}}^{\mathbb{D}_{\text{or}}^i}$, and then the data routing under the DSDR scheme can be described by Algorithm 2.

5. Performance Analysis of DSDR

In this section, the effectiveness of DSDR scheme is analyzed from three aspects: network delay, energy efficiency, and network lifetime. At the same time, the performance of DSDR scheme is compared with the General Data Routing Approach (DR-GA), which is a routing scheme based on the shortest distance and multihop relaying. Without additional descriptions, the network parameters are set as follows: $R = 500$, $r = 80$, and $\rho = 0.1$, and for values for other parameters please see Table 1.

5.1. Transmission Delay. According to [17], suppose that ς_d^i is the node whose distance to the sink is i, its communication duty cycle is ϕ_{C}^i, communication cycle is $\mathcal{T}_{\text{COM}}$, and then the one-hop transmission delay of ς_d^i can be expressed as follows:

$$D_{\text{ONE}}^i = \left(1 - \phi_{\text{C}}^i\right)^2 \frac{\mathcal{T}_{\text{COM}}}{2} + d_{\text{Pr}} + d_{\text{Da}} + d_{\text{Ac}}. \quad (15)$$

In DR-GA, suppose that ς_d^i is the node whose distance to the sink is i, its communication radius is r, and then the relay hops from ς_d^i to the sink are $\lceil i/r \rceil$. Therefore, the end-to-end transmission delay from ς_d^i to the sink is the product of the relay hops and one-hop delay; that is,

$$D_{E2E}^i = \left\lceil \frac{i}{r} \right\rceil \left[\left(1 - \phi_{\text{C}}^i\right)^2 \frac{\mathcal{T}_{\text{COM}}}{2} + d_{\text{Pr}} + d_{\text{Da}} + d_{\text{Ac}} \right]. \quad (16)$$

In DSDR, one-hop delay varies depending on the different types of data, suppose that $\mathbb{D}_{\text{ds}}$ are delay-sensitive data and $\mathbb{D}_{\text{or}}$ are delay-tolerant data, and then the one-hop delay of them can be calculated by Theorems 3 and 4.

Theorem 3. *In DSDR, suppose that ς_d^i is the node whose distance to the sink is i, the data it transferred is $\mathbb{D}_{ds}$,*

(1) **For** each node ς_{tr} sensed data **Do**
(2) **If** $\varsigma_{tr.}\mathcal{Q}_{tS} = 1$ **then**
(3) ς_{tr} sends data to the sink directly
(4) **End if**
(5) **Else if** $\varsigma_{tr.}\varphi^{e}$ = true **then**
(6) **While** $\varsigma_{tr.}\mathcal{Q}_{tR} > 0$ **Do**
(7) ς_{tr} transmits data to ς_{next}: $\varsigma_{\text{next.}}\mathcal{Q}_{tR} < \varsigma_{tr.}\mathcal{Q}_{tR}$
(8) Let $\varsigma_{tr} = \varsigma_{\text{next}}$
(9) **End while**
(10) **While** $\varsigma_{tr.}\mathcal{Q}_{tS} > 0$ **Do**
(11) ς_{tr} transmits data to ς_{next}: $\varsigma_{\text{next.}}\mathcal{Q}_{tS} < \varsigma_{tr.}\mathcal{Q}_{tS}$ and $\varsigma_{\text{next.}}\mathcal{Q}_{tR} = 0$
(12) Let $\varsigma_{tr} = \varsigma_{\text{next}}$
(13) **End while**
(14) **End else**
(15) **Else if** $\varsigma_{tr.}\varphi^{e}$ = false **then**
(16) **While** $\varsigma_{tr.}\mathcal{Q}_{tR} > 0$ **Do**
(17) ς_{tr} transmits data to ς_{next}: $\varsigma_{\text{next.}}\mathcal{Q}_{tR} < \varsigma_{tr.}\mathcal{Q}_{tR}$
(18) Data stops at ς_{next} for $T_{\text{one}}^{\mathbb{D}_{\text{or}}^{i}}$ for data fusion
(19) Let $\varsigma_{tr} = \varsigma_{\text{next}}$
(20) **End while**
(21) **While** $\varsigma_{tr.}\mathcal{Q}_{tS} > 0$ **Do**
(22) ς_{tr} transmits data to ς_{next}: $\varsigma_{\text{next.}}\mathcal{Q}_{tS} < \varsigma_{tr.}\mathcal{Q}_{tS}$ and $\varsigma_{\text{next.}}\mathcal{Q}_{tR} = 0$
(23) Data stops at ς_{next} for $T_{\text{one}}^{\mathbb{D}_{\text{or}}^{i}}$ for data fusion
(24) Let $\varsigma_{tr} = \varsigma_{\text{next}}$
(25) **End while**
(26) **End else**
(27) **End for**

Algorithm 2: Data routing under DSDR scheme.

its communication duty cycle is ϕ_C^i, communication cycle is $\mathcal{T}_{\text{COM}}$, if ς_d^i is the far-sink node on E2RPs then F_{RP}^f is true, and then the one-hop delay of ς_d^i can be expressed as follows:

$$D_{1\_hop}^{i}(\mathbb{D}_{ds}) = \begin{cases} \left(1-\phi_C^i\right)^2 \dfrac{\mathcal{T}_{\text{COM}}}{2} + d_{Pr} + d_{Da} + d_{Ac} & \text{if } F_{RP}^f = \text{false} \\ d_{Pr} + d_{Da} + d_{Ac} & \text{if } F_{RP}^f = \text{true.} \end{cases} \quad (17)$$

Proof. Nodes have different one-hop delay due to different types. When ς_d^i is an ordinary node of the far-sink area or a near-sink node, its parameter values are not adjusted. Its one-hop delay is the same as that of the DR-GA. However, if ς_d^i is the far-sink node on E2RPs, because the communication duty cycles of nodes on E2RPs are 1, they have no $(1-\phi_C^i)^2(\mathcal{T}_{\text{COM}}/2)$ delay. The one-hop delay is $d_{\text{Pr}} + d_{\text{Da}} + d_{\text{Ac}}$. d_{Pr} is the packet preamble receiving delay, d_{Da} is the data communication delay, and d_{Ac} is the acknowledgment message transmission delay. □

Theorem 4. *In DSDR, suppose that ς_d^i is the node whose distance to the sink is i, the data it transferred is $\mathbb{D}_{or}$, its waiting duration at each relay is $T_{one}^{\mathbb{D}_{or}^{i}}$, if ς_d^i is the far-sink node on E2RPs then F_{RP}^f is true, and then the one-hop delay of ς_d^i can be expressed as follows:*

$$D_{1\_hop}^{i}(\mathbb{D}_{or}) = \begin{cases} \left(1-\phi_C^i\right)^2 \dfrac{\mathcal{T}_{\text{COM}}}{2} + d_{Pr} + d_{Da} + d_{Ac} + T_{one}^{\mathbb{D}_{\text{or}}^{i}} & \text{if } F_{RP}^f = \text{false} \\ d_{Pr} + d_{Da} + d_{Ac} + T_{one}^{\mathbb{D}_{or}^{i}} & \text{if } F_{RP}^f = \text{true.} \end{cases} \quad (18)$$

Proof. When the data transmitted is $\mathbb{D}_{\text{or}}$, its one-hop delay is divided into two cases: (1) ς_d^i is an ordinary node of the far-sink area or a near-sink node. (2) ς_d^i is the far-sink node on E2RPs. The delay of the two cases is similar to (17). However, delay-tolerant data are delayed $T_{\text{one}}^{\mathbb{D}_{\text{or}}^{i}}$ time at each relay hop, and the delay of delay-tolerant data is $T_{\text{one}}^{\mathbb{D}_{\text{or}}^{i}}$ more than that of delay-sensitive data. Therefore, (18) is proved. □

Theorem 5. *In DSDR, suppose that ς_d^i is the node whose distance to the sink is i, its minimum hops to the sink are $\varsigma_{d.}^{i}\mathcal{Q}_{tS}$, its hops to nearest E2RP are $\varsigma_{d.}^{i}\mathcal{Q}_{tR}$, and the hops from* E2RP *to the sink are $\mathcal{Q}_{R2S}^{j}$. If ς_d^i is the node in near-sink area then F_{ς_i} is 0, if ς_d^i is the node in far-sink area and its transmitted data is $\mathbb{D}_{ds}$ then F_{ς_i} is 1, if ς_d^i is the node in far-sink area and its transmitted data is $\mathbb{D}_{or}$ then F_{ς_i} is −1, and then the end-to-end delay from ς_d^i to the sink can be expressed as follows:*

$$D_{e2e}^{i} = \begin{cases} \varsigma_{d.}^{i} \mathcal{Q}_{tS} \left[\left(1 - \phi_C^i\right)^2 \frac{\mathcal{T}_{\mathrm{COM}}}{2} + \mu_d \right] & \text{if } F_{\varsigma_i} = 0 \\ \frac{\left(1 - \phi_C^i\right)^2 \left(\varsigma_{d.}^{i} \mathcal{Q}_{tR} + 1\right) \mathcal{T}_{\mathrm{COM}}}{2} + \mu_d \left(\varsigma_{d.}^{i} \mathcal{Q}_{tR} + \mathcal{Q}_{R2S}^{j}\right) & \text{if } F_{\varsigma_i} = 1 \\ \frac{\left(1 - \phi_C^i\right)^2 \left(\varsigma_{d.}^{i} \mathcal{Q}_{tR} + 1\right) \mathcal{T}_{\mathrm{COM}}}{2} + \left(\varsigma_{d.}^{i} \mathcal{Q}_{tR} + \mathcal{Q}_{R2S}^{j}\right) \left(\mu_d + T_{one}^{\mathbb{D}_{or}^{i}}\right) & \text{if } F_{\varsigma_i} = -1, \end{cases} \tag{19}$$

where $\mu_d = d_{Pr} + d_{Da} + d_{Ac}$.

Proof. In DSDR, the transmission delay of ς_d^i is divided into three situations depending on the network locations and data types. (1) When ς_d^i is a node in near-sink area, then the data is sent directly to the sink regardless of the data type. Therefore, its end-to-end delay is the product of the one-hop delay and relay hops: $\varsigma_{d.}^{i} \mathcal{Q}_{tS}[(1 - \phi_C^i)^2(\mathcal{T}_{\mathrm{COM}}/2) + \mu_d]$. (2) When ς_d^i is a node in far-sink area and the data it transferred is $\mathbb{D}_{\mathrm{ds}}$, its delay is divided into two phases: delay from ς_d^i to E2RP and delay from E2RP to the sink. Delay in the previous phase is the product of one-hop delay and hops from ς_d^i to E2RP: $\varsigma_{d.}^{i} \mathcal{Q}_{tR}[(1 - \phi_C^i)^2(\mathcal{T}_{\mathrm{COM}}/2) + \mu_d]$. Delay in the latter part is also divided into two cases. Because the duty cycles of far-sink nodes on the E2RP are 1 and the duty cycles of near-sink nodes remain unchanged, the delay in this phase is divided into a partial delay from E2RP to near-sink node (the duty cycle is 1) and the one-hop delay from near-sink node to the sink (the original duty cycle). The delay of the previous part is $\mu_d(\mathcal{Q}_{R2S}^{j} - 1)$, followed by a delay of $(1 - \phi_C^i)^2(\mathcal{T}_{\mathrm{COM}}/2) + \mu_d$. (3) When ς_d^i is a node in far-sink area and the data it transferred is $\mathbb{D}_{\mathrm{or}}$, its delay is divided into two cases similar to $\mathbb{D}_{\mathrm{ds}}$, but delay-tolerant data wait for $T_{\mathrm{one}}^{\mathbb{D}_{\mathrm{or}}^{i}}$ at each relay, so its delay is $T_{\mathrm{one}}^{\mathbb{D}_{\mathrm{or}}^{i}}(\varsigma_{d.}^{i} \mathcal{Q}_{tR} + \mathcal{Q}_{R2S}^{j})$ more than delay-sensitive data. □

Definition 6. Total network delay (denoted as D_{tot}) refers to the sum of transmission delays of the entire network. Since the transmission delay is distinct for different distances from the sink, hence, D_{tot} is determined by integrating the transmission delays of different regions. Suppose that ς_d^i is the node whose distance to the sink is i, its end-to-end delay is D_{e2e}^{i}, taking an arbitrary annular area with the distance from the sink $i \mid i \in \{0, \ldots, R\}$, the width of di, and the angle of $d\theta$, then the delay of this region is $D_{e2e}^{i} i di d\theta$, and, therefore, the delay of the entire network can be expressed as

$$D_{\mathrm{tot}} = \int_0^R \int_0^{2\pi} D_{e2e}^{i}\, i\, di\, d\theta. \tag{20}$$

Figures 12–16 show the transmission delays in DR-GA and DSDR. Figure 12 is the one-hop delay of them. In DR-GA, the one-hop delay of all nodes is the same due to the constant parameter values. In DSDR, the one-hop delay of nodes that transmit delay-sensitive data is divided into two cases. After the data reach the E2RP, the communication duty cycles of relay nodes are 1 and the delay is small; otherwise the one-hop delay of the nodes is the same as that in DR-GA. The delay of delay-tolerant data in DSDR is similar to that of delay-sensitive data, but the nodes stay for a short period of time for data fusion at each relay, so the delay is larger than the delay-sensitive data.

Figure 13 shows the end-to-end delay under DR-GA scheme. It can be seen that the transmission delay increases rapidly with the distance from the sink, and the maximum delay in the network is about 4–6 times the minimum delay.

Figure 14 shows the end-to-end delay for different types of data under DSDR scheme. As can be seen from the figure, (1) transmission delay of the delay-sensitive data is much smaller than that of delay-tolerant data and (2) delay in the far-sink area is greatly reduced by transmitting data via E2RPs, and the maximum delay in the network is about 2.5 times the minimum delay. Combining Figures 13 and 14 it can be seen that DSDR scheme has a significant advantage in reducing transmission delay when comparing with DR-GA scheme.

Figures 15 and 16 show the transmission delay at different duty cycles and communication radius under DR-GA and DSDR scheme. As can be seen from Figure 15, when the node duty cycle is 0.2, the transmission delay under the DSDR scheme is much lower than the DR-GA, which means that the DSDR can improve the transmission speed with less energy cost. And as shown in Figure 16, obviously, compared with the DR-GA scheme, the DSDR scheme proposed in this paper has high efficiency in transmitting both delay-sensitive data and delay-tolerant data, especially in the transmission of delay-sensitive data, and it can reduce the delay by 44.31%.

5.2. Energy Utilization. According to (11), in DR-GA, suppose that ς_d^i is the node whose distance to the sink is i, its communication radius is r, the probability of generating data is P_d, and then the number of packets received by ς_d^i is $[(Z + 1) + Z(Z+1)r/2i]P_d$, where Z is the largest positive integer that makes the expression $i + Zr < R$ true. The number of packets transmitted by ς_d^i is the sum of the packets received and the packets it generated, and it can be expressed as follows:

$$\Pi_T^i = \left[(Z + 1) + \frac{Z(Z + 1)\, r}{2i} \right] P_d + P_d \quad \text{where } i + Zr < R. \tag{21}$$

Similarly, according to (12), in DSDR, suppose that ς_d^i is the node whose distance to the sink is i, the distance from ς_d^i

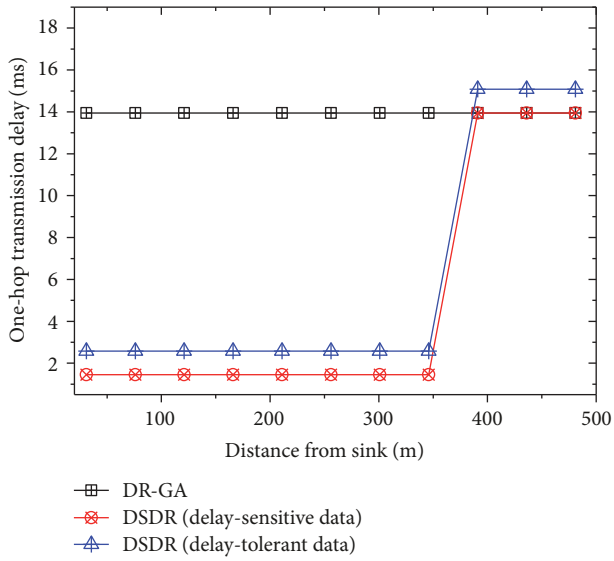

Figure 12: One-hop delay in DR-GA and DSDR.

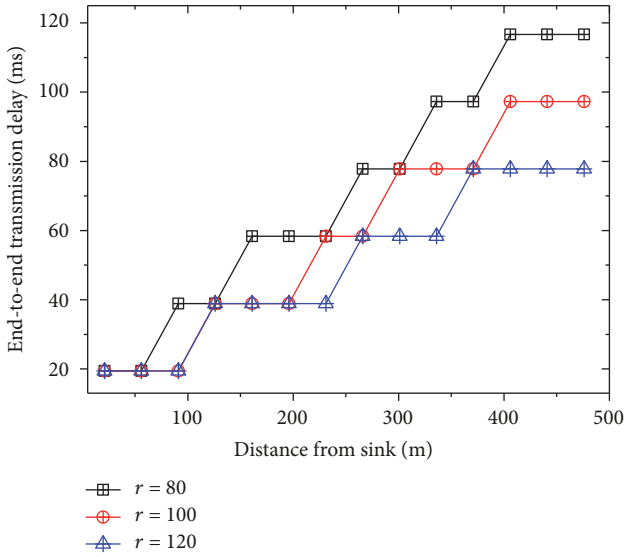

Figure 13: End-to-end transmission delay in DR-GA.

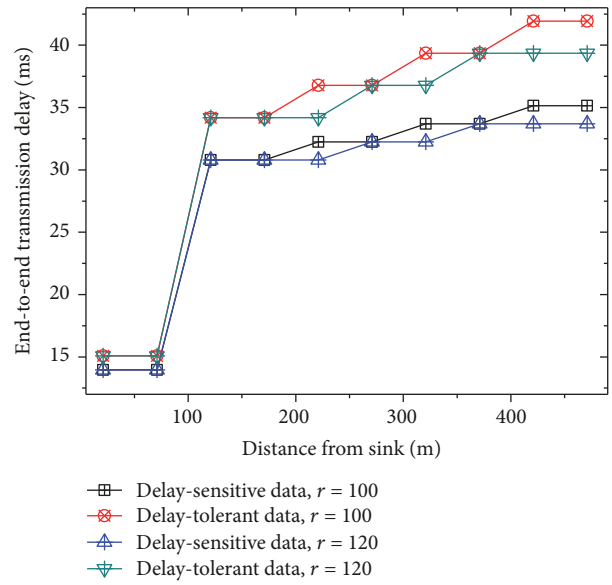

Figure 14: End-to-end delay for different data in DSDR.

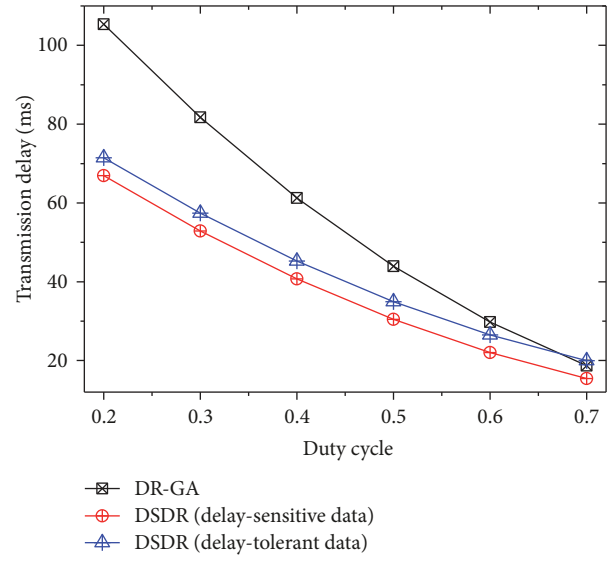

Figure 15: Transmission delay for different duty cycles under DR-GA and DSDR.

to its nearest E2RP is K_e^i, and the number of packets received by ς_d^i is $\max([(Z+1)+Z(Z+1)r/2i]P_d, [(Z+1)+Z(Z+1)r/2K_e^i]P_d)$, and then the number of packets transmitted by ς_d^i can be expressed as follows:

$$\Pi_{\text{Tra}}^i = \max\left(\left[(Z+2)+\frac{Z(Z+1)r}{2i}\right]P_d, \left[(Z+2)+\frac{Z(Z+1)r}{2K_e^i}\right]P_d\right) \quad \text{where } i+Zr<R. \tag{22}$$

Theorem 7. *In DSDR, the direct-forwarding is adopted for delay-sensitive data and wait-forwarding is adopted for delay-tolerant data, and suppose that ς_d^i is the node whose distance to the sink is i, and the number of packets received by ς_d^i is Π_{Rec}^i, where μ_d stands for delay-sensitive data, the packet length of delay-sensitive data is δ_d and the packet length of delay-tolerant data is δ_o, and $\mathscr{E}_\lambda = 1-\lambda_\vartheta$, where λ_ϑ is the correlation coefficient of data, and the data has passed k hops*

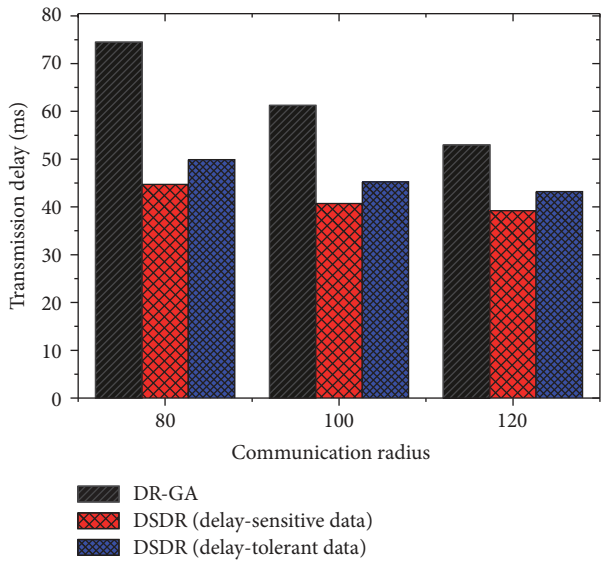

FIGURE 16: Transmission delay for different communication radius under DR-GA and DSDR.

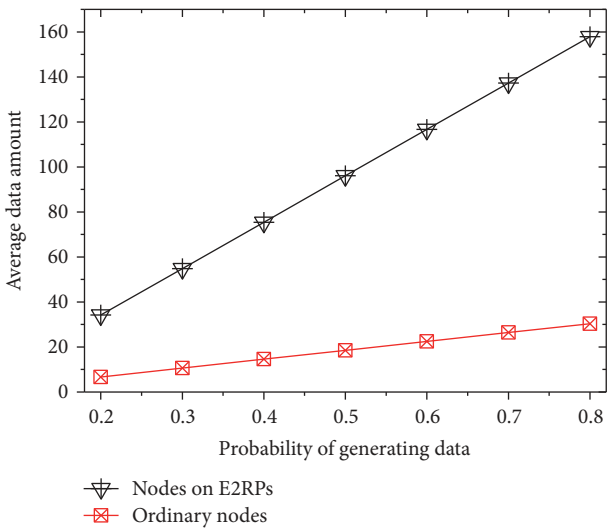

FIGURE 17: Data amount for different nodes.

before relaying to ς_d^i*, and then the amount of data received by* ς_d^i *can be expressed as follows:*

$$\varphi_{Rec}^i = \Pi_{Rec}^i \mu_d \delta_d + \delta_o \left\{ \left(\mathscr{E}_\lambda\right)^k \left[\Pi_{Rec}^i \left(1-\mu_d\right)\right] + 1 \right\}. \quad (23)$$

Proof. The amount of data received by ς_d^i is divided into the amount of delay-sensitive data and the amount of delay-tolerant data. Since μ_d of Π_{Rec}^i is delay-sensitive data, the number of delay-sensitive packets is $\Pi_{\text{Rec}}^i \mu_d$, the length of each delay-sensitive packet is δ_d, and, therefore, the amount of delay-sensitive data received by ς_d^i is $\Pi_{\text{Rec}}^i \mu_d \delta_d$. And delay-tolerant data are fused at each hop, suppose that the data has passed k hops before it relays to ς_d^i, then the data packets after data fusion can be obtained according to (14), and the amount of delay-tolerant data received by ς_d^i is the product of data packets after data fusion and the length of each packet. □

The amount of data transmitted by ς_d^i can be obtained by fusing the received delay-tolerant data once again:

$$\varphi_{\text{Tran}}^i = \Pi_{\text{Tra}}^i \mu_d \delta_d + \delta_o \left\{ \left(\mathscr{E}_\lambda\right)^{k+1} \left[\Pi_{\text{Tra}}^i \left(1-\mu_d\right)\right] + 1 \right\}. \quad (24)$$

Definition 8. Average data amount of an E2RP (denoted as φ_{RP}) refers to the average data amount borne by each E2RP, including the receiving data amount and transmitting data amount. Since E2RPs only forward the data of far-sink area, therefore, φ_{RP} is the quotient of the total data amount of the far-sink area and the total number of E2RPs. Suppose that the node from the sink i is ς_d^i, the data amount of ς_d^i is φ_i, and there are N_{RP} E2RPs in the network, taking an arbitrary annular area with the distance from the sink $i \mid i \in \{0, \ldots, R\}$, the width of di, and the angle of $d\theta$, and then the data amount of the far-sink area can be obtained by integrating the area with the radius of r-R and the angle of 0-2π. Consequently, the average data amount of an E2RP can be expressed as

$$\varphi_{\text{RP}} = \frac{\int_r^R \int_0^{2\pi} \varphi_i \, i \, di \, d\theta}{N_{\text{RP}}}. \quad (25)$$

Figure 17 shows the data amount of different nodes in the far-sink area under the DSDR scheme. As we can see from the figure, (1) because the nodes on E2RPs are expected to forward data from the nearby far-sink area, their data amount is much higher than ordinary nodes', which are about 5 times. (2) The data amount of each node in the network increases gradually with the increase of the duty cycle, especially the nodes on E2RPs.

Equation (4) is the energy consumption model: $E_{\varsigma_i} = \epsilon_{\text{Se}}^i + \epsilon_{\text{Td}}^i + \epsilon_{\text{Rd}}^i + \epsilon_{\text{Lp}}^i$, where ϵ_{Se}^i is the energy consumption in event sensing, ϵ_{Td}^i is the energy consumption in data transmission, ϵ_{Rd}^i is the energy consumption in data receiving, and ϵ_{Lp}^i is the energy consumption in low power listening. Energy consumption in data transmission and data receiving is closely related to the data amount, and when the data amount is large, the energy consumption of nodes is serious.

According to [17], suppose that the node communication duty cycle is ϕ_C, communication cycle is $\mathscr{T}_{\text{COM}}$, and then the energy consumption to transmit a packet can be expressed as follows:

$$\epsilon_{\text{Td}}^{\text{one}} = \left[\frac{\phi_C \mathscr{T}_{\text{COM}}}{4\left(d_{\text{Pr}} + d_{\text{Ac}}\right)} + \frac{1}{2} \right] \left(\mathscr{E}_T d_{\text{Pr}} + \mathscr{E}_R d_{\text{Ac}}\right) + \mathscr{E}_T d_{\text{Da}}. \quad (26)$$

The first item is the transmission consumption to notify the receiving node of the periodic preamble when the packet arrives, and $\mathscr{E}_T d_{\text{Da}}$ is the data transmission consumption.

With the same duty cycle and communication cycle, the energy consumption to receive a packet can be expressed as follows:

$$\epsilon_{\mathrm{Rd}}^{\mathrm{one}} = \mathscr{E}_R d_{\mathrm{Pr}} + \mathscr{E}_R d_{\mathrm{Da}} + \mathscr{E}_T d_{\mathrm{Ac}}, \tag{27}$$

where $\mathscr{E}_R d_{\mathrm{Pr}}$ is the energy consumption to receive sequences, $\mathscr{E}_R d_{\mathrm{Da}}$ is the energy consumption to receive data, and $\mathscr{E}_T d_{\mathrm{Ac}}$ is the energy consumption to transmit the acknowledgment messages to the sending node.

The energy consumption of event sensing is composed of its sleep consumption and sensing consumption. Suppose that the sensing duty cycles of nodes are ϕ_S, the power consumption of event sensing is $\mathscr{E}_{\mathrm{Se}}$, and the power consumption of sleeping is $\mathscr{E}_{\mathrm{Sl}}$, and then the energy consumption of nodes in a sensing cycle of $\mathscr{T}_{\mathrm{SEN}}$ can be expressed as follows:

$$\epsilon_{\mathrm{Se}}^{\mathscr{T}_{\mathrm{SEN}}} = \left[\mathscr{E}_{\mathrm{Se}}\phi_S + \mathscr{E}_{\mathrm{Sl}}\left(1-\phi_S\right)\right]\mathscr{T}_{\mathrm{SEN}}. \tag{28}$$

The energy consumption of low power listening is relatively small, according to [14], suppose that ς_d^i is the node whose distance to the sink is i, its communication duty cycle is ϕ_C^i, communication cycle is $\mathscr{T}_{\mathrm{COM}}$, and then the energy consumption of ς_d^i in low power listening can be expressed as follows:

$$\epsilon_{\mathrm{Lp}}^i = \left[\mathscr{E}_R\phi_C^i + \mathscr{E}_{\mathrm{Sl}}\left(1-\phi_C^i\right)\right]\mathscr{T}_{\mathrm{COM}} - \mathfrak{T}_T^i - \mathfrak{T}_R^i. \tag{29}$$

The energy consumption of nodes in low power listening consists of listening consumption and sleeping consumption, that is, $[\mathscr{E}_R\phi_C^i + \mathscr{E}_{\mathrm{Sl}}(1-\phi_C^i)]\mathscr{T}_{\mathrm{COM}}$, but it is required to subtract the consumption of $\mathfrak{T}_T^i$ and $\mathfrak{T}_R^i$ that have been calculated in data transmission and receiving.

The calculations for $\mathfrak{T}_T^i$ and $\mathfrak{T}_R^i$ in (29) are given in [14, 43], as shown in

$$\mathfrak{T}_T^i = \left\{\left[\frac{\left(1-\phi_C^i\right)\mathscr{T}_{\mathrm{COM}}}{2} + d_{\mathrm{Pr}} + d_{\mathrm{Ac}}\right]\mathscr{E}_{\mathrm{Sl}} + \mathscr{E}_R d_{\mathrm{Pr}}\right\}\frac{\varphi_{\mathrm{Tra}}^i}{\mathscr{T}_{\mathrm{COM}}} \tag{30}$$

$$\mathfrak{T}_R^i = \left[\left(d_{\mathrm{Da}} + d_{\mathrm{Ac}}\right)\mathscr{E}_{\mathrm{Sl}} + \mathscr{E}_R d_{\mathrm{Pr}}\right]\frac{\varphi_{\mathrm{Rec}}^i}{\mathscr{T}_{\mathrm{COM}}}.$$

At this point, the energy consumption of each part for the node has been given. According to the energy consumption model of this paper, suppose that ς_d^i is the node whose distance to the sink is i, and then the energy consumption of ς_d^i under the DSDR scheme can be expressed as follows:

$$E_{\varsigma_d^i} = \epsilon_{\mathrm{Se}}^i + \epsilon_{\mathrm{Td}}^i\varphi_{\mathrm{Tra}}^i + \epsilon_{\mathrm{Rd}}^i\varphi_{\mathrm{Rec}}^i + \epsilon_{\mathrm{Lp}}^i. \tag{31}$$

Figures 18–20 show the energy consumption under DR-GA and DSDR. Among them, Figures 18 and 19 describe the energy consumption corresponding to different duty cycles under DR-GA and DSDR, respectively. As shown in Figure 18, the energy consumption under DR-GA decreases gradually

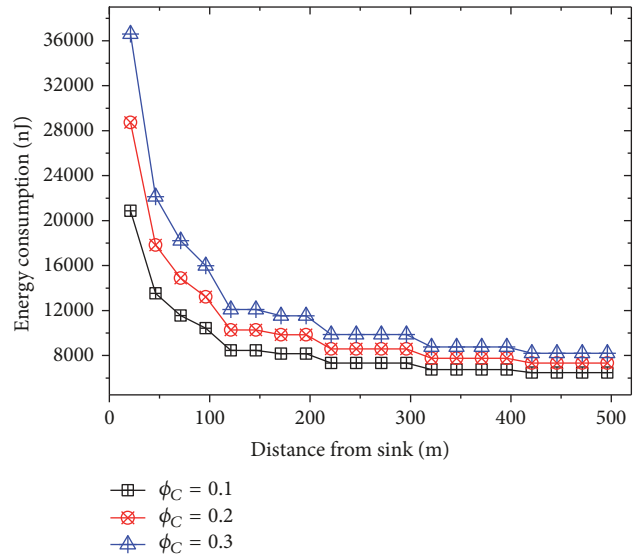

Figure 18: Energy consumption under DR-GA.

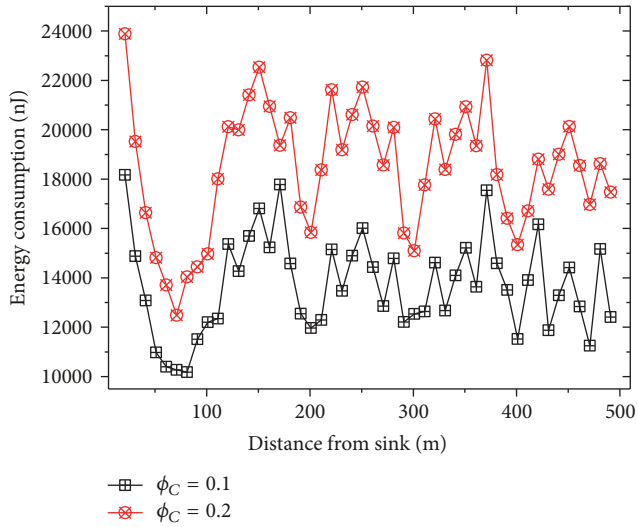

Figure 19: Energy consumption under DSDR.

with the distance from the sink, and the energy consumption of near-sink area is serious, while the consumption of far-sink are is slight, and the maximum energy consumption in the network is about 3 times the minimum energy consumption, which indicates that the energy consumption under DR-GA is not balanced. While, in the DSDR scheme shown in Figure 19, the energy consumption of the entire network is much more balanced, the maximum energy consumption in the network is less than twice the minimum, and the energy consumption of the entire network presents such a law: the energy consumption of regions near the sink or E2RPs is serious, and it decreases with the distance from them. However, whether DR-GA or DSDR, the node with the most serious energy consumption is still the node closest to the sink, and the maximum energy consumption in DSDR

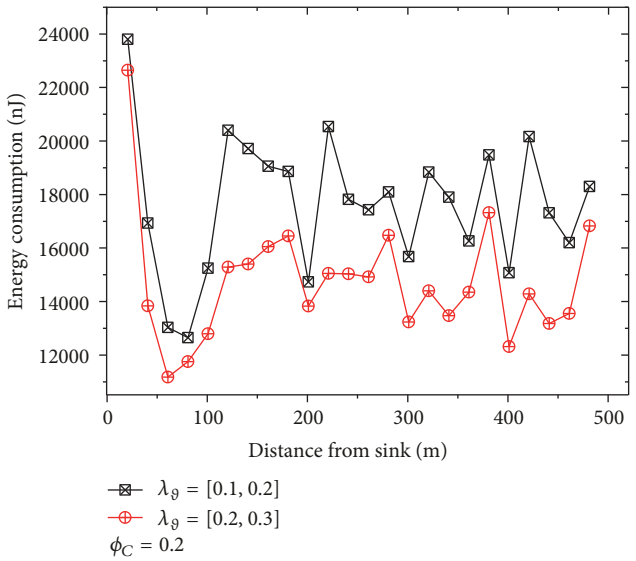

Figure 20: Energy consumption under different data relevance.

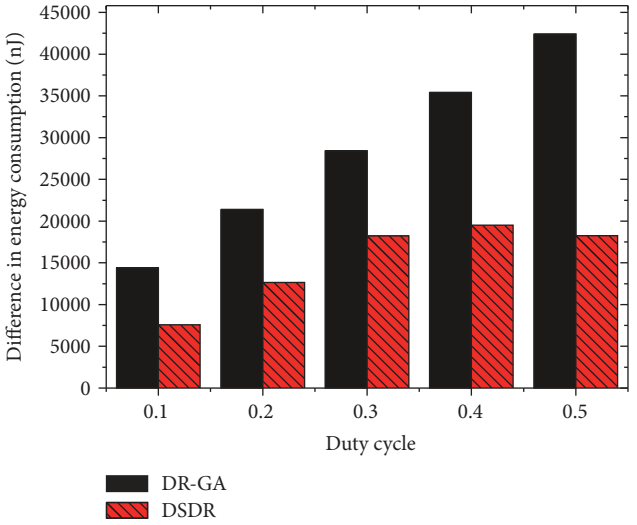

Figure 21: Energy consumption difference in DR-GA and DSDR.

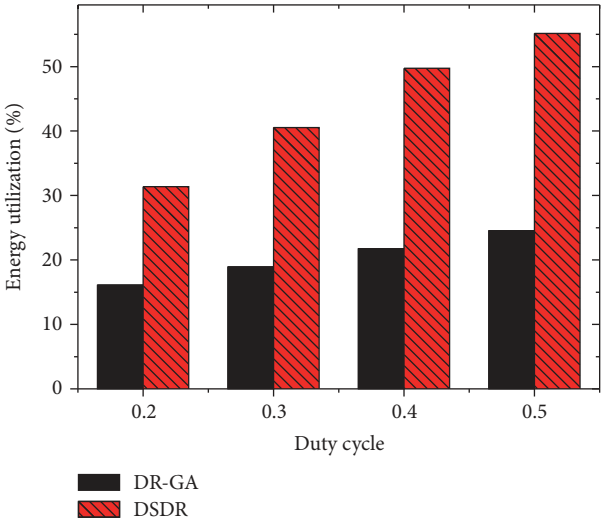

Figure 22: Energy utilization in DR-GA and DSDR.

is slightly smaller than DR-GA due to the reduction of redundancy by data fusion, which also shows the efficiency of DSDR.

Figure 20 shows the energy consumption of different data relevance under the DSDR scheme, where λ_ϑ is the correlation coefficient of data. Since λ_ϑ directly affects the data fusion rate, when λ_ϑ is larger, the data can be fused to a greater degree, then the data amount needs to be transmitted is reduced, and the energy consumed by data forwarding is less. As shown in Figure 20, when λ_ϑ is between 0.2 and 0.3, its energy consumption is much smaller than it is between 0.1 and 0.2.

Definition 9. Energy difference (denoted as E_{dif}) refers to the difference of the maximum energy consumption and the minimum energy consumption in the network. Suppose there are N nodes in the network, the kth node is denoted as ς_k, and the energy consumed by ς_k is E_{ς_k}, and then the calculation of E_{dif} is depicted as

$$E_{\text{dif}} = \max_{1\le k\le N} \left(E_{\varsigma_k}\right) - \min_{1\le k\le N} \left(E_{\varsigma_k}\right). \tag{32}$$

Definition 10. Energy utilization (denoted as $\mathcal{R}_{e\_\text{uti}}$) refers to the ratio of the total energy consumed by the network when the network dies to the total initial energy of the network, which is determined by the quotient of the energy consumed by all nodes and the initial energy of all nodes. Suppose there are N nodes in the network, the kth node is denoted as ς_k, and the energy consumed by ς_k is E_{ς_k}, the initial energy of ς_k is $\overline{E}_{\text{Ini}}$, and then the calculation of $\mathcal{R}_{e\_\text{uti}}$ is depicted as

$$\mathcal{R}_{e\_\text{uti}} = \frac{\sum_{k=1}^{N} E_{\varsigma_k}}{\sum_{k=1}^{N} \overline{E}_{\text{Ini}}}. \tag{33}$$

Figure 21 is the energy consumption difference under DSDR and DR-GA, and the smaller the difference is, the more balanced the energy consumption is; otherwise it shows that the energy of some area in the network is not fully utilized. It is clear that compared with DR-GA the DSDR proposed in this paper has a lower energy difference, which shows that the energy consumption under DSDR is more balanced. Figure 22 shows the energy utilization of DSDR and DR-GA. Compared with DR-GA, the DSDR can improve the energy utilization by 30.61%, and especially when the duty cycle is large it has significant advantages in energy utilization.

5.3. Network Lifetime

Definition 11. Network lifetime (denoted as $\mathcal{F}_\ell$) refers to the time intervals from the time when the network is established to the time when the network is dead, which is defined as the death time of the first node in the network, where the death of nodes resulted from exhausted battery energy. Suppose there

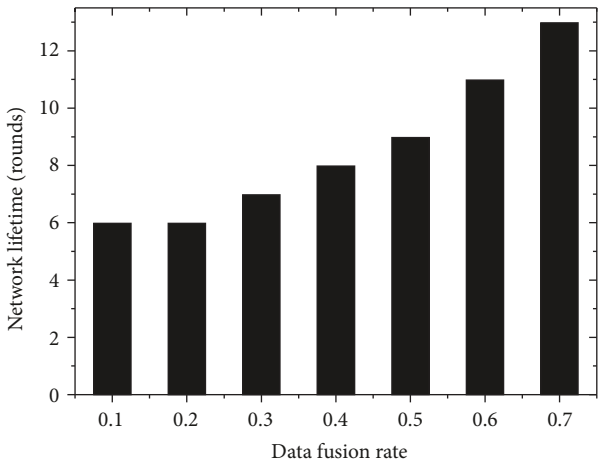

Figure 23: Network lifetime under different data fusion rate.

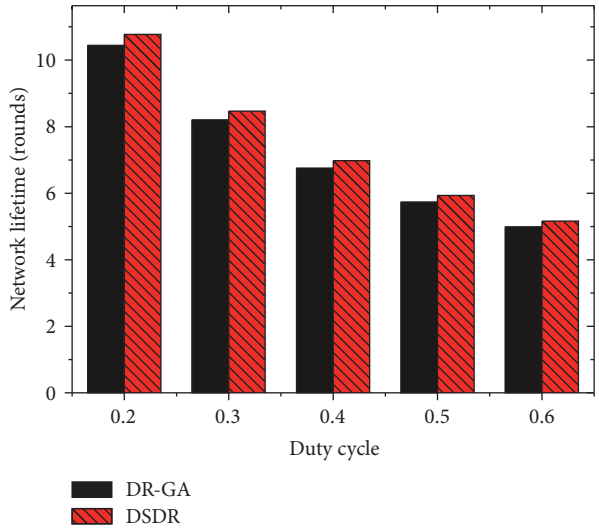

Figure 24: Network lifetime in DR-GA and DSDR.

are N nodes in the network, the kth node is denoted as ς_k, and the energy consumed by ς_k is E_{ς_k}, the initial energy of ς_k is $\overline{E}_{\text{Ini}}$, and then the $\mathcal{F}_\ell$ is depicted as

$$\mathcal{F}_\ell = \frac{\overline{E}_{\text{Ini}}}{\max_{1\le k\le N} E_{\varsigma_k}}. \tag{34}$$

Figure 23 shows the network lifetime under different data fusion rate, and the higher the data fusion rate is, the less data are needed to transmit, the less energy the nodes consume, and the longer the network lifetime is.

Figure 24 is the lifetime comparison of DSDR and DR-GA, although the energy utilization greatly improved under DSDR scheme, the increasing consumption has no impact on network lifetime. What is more, it makes the lifetime have a certain improvement. This is explained by the fact that, under the DSDR proposed in this paper, we choose different routings for different areas. In the far-sink area we use E2RPs to transmit data and switch the E2RPs intelligently, so the energy consumption of E2RPs in far-sink area will only enhance energy utilization and do not affect the maximum energy consumption of the network. For the near-sink area we retain the original data routing mode, and the near-sink nodes are often the nodes that affect the entire network lifetime, under the condition that the energy consumption of these nodes is constant, and the lifetime of the network remains unchanged. In addition, data redundancy is reduced by data fusion, so the maximum energy consumption under DSDR is smaller than that of DR-GA.

5.4. Effect of Other Parameters on the Performance

(1) The Proportion of Delay-Sensitive Data

Theorem 12. *Suppose that there are N_f nodes in the far-sink area of the network, the kth node is denoted as ς_k, and the data amount of ς_k is φ_{ς_k}, where μ_d^k stands for delay-sensitive data, the transmission delay for delay-sensitive data is D_{ds}^k, and the transmission delay for delay-tolerant data is $D_{or}^k (D_{ds}^k < D_{or}^k)$, and then the average transmission delay of far-sink area can be expressed as follows:*

$$D_{avg}^f = \frac{\sum_{1\le k\le N_f} \left[\varphi_{\varsigma_k}\mu_d^k D_{ds}^k + \varphi_{\varsigma_k}\left(1-\mu_d^k\right) D_{or}^k\right]}{N_f}. \tag{35}$$

Proof. The transmission delay of ς_k is composed of the transmission delay of delay-sensitive data and the transmission delay of delay-tolerant data. Because the delay for the delay-sensitive packet is D_{ds}^k, and the proportion of the delay-sensitive data to the data amount is μ_d^k, then the delay of delay-sensitive data is $\varphi_{\varsigma_k}\mu_d^k D_{\text{ds}}^k$. Correspondingly, the delay of delay-tolerant data is $\varphi_{\varsigma_k}(1-\mu_d^k)D_{\text{or}}^k$. The average transmission delay of far-sink area is obtained by dividing the total delays into the number of nodes. □

Similar to Theorem 12, suppose that there are N_f nodes in the far-sink area of the network, the kth node is denoted as ς_k, and the data amount of ς_k is φ_{ς_k}, where μ_d^k stands for delay-sensitive data, the energy consumption to transmit a delay-sensitive packet is $€_{\text{Td\_ds}}^k$, the energy consumption to transmit a delay-tolerant packet is $€_{\text{Td\_or}}^k (€_{\text{Td\_ds}}^k > €_{\text{Td\_or}}^k)$, and then the average energy consumption of far-sink area can be expressed as follows:

$$E_{\text{avg}}^f = \frac{\sum_{1\le k\le N_f} \left[\varphi_{\varsigma_k}\mu_d^k €_{\text{Td\_ds}}^k + \varphi_{\varsigma_k}\left(1-\mu_d^k\right) €_{\text{Td\_or}}^k\right]}{N_f}. \tag{36}$$

Figures 25 and 26 show the transmission delay and energy consumption at different proportion of delay-sensitive data under DSDR scheme. In Figure 25, because the delay of delay-sensitive data is less than delay-tolerant data, then the higher the proportion of delay-sensitive data is, the smaller the average transmission delay of the network is. In Figure 26, the greater the proportion of delay-sensitive data is, the more the serious energy the network consumes, because the delay-tolerant data are transmitted after data fusion and the data redundancy is greatly reduced, so energy consumption of

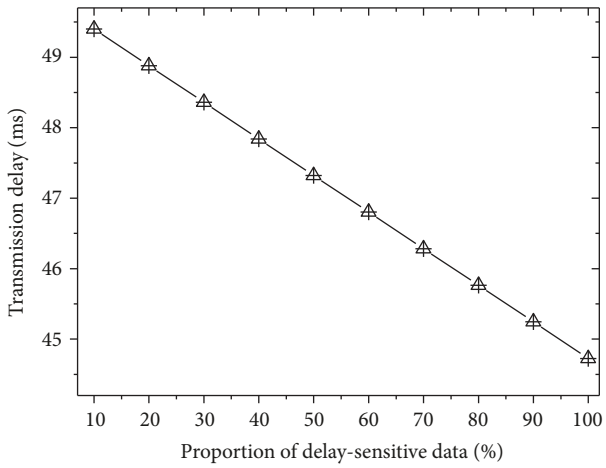

Figure 25: Transmission delay under different proportion of delay-sensitive data.

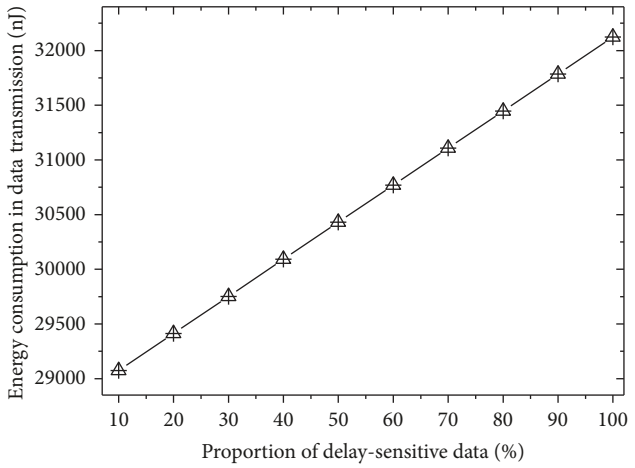

Figure 26: Energy consumption under different proportion of delay-sensitive data.

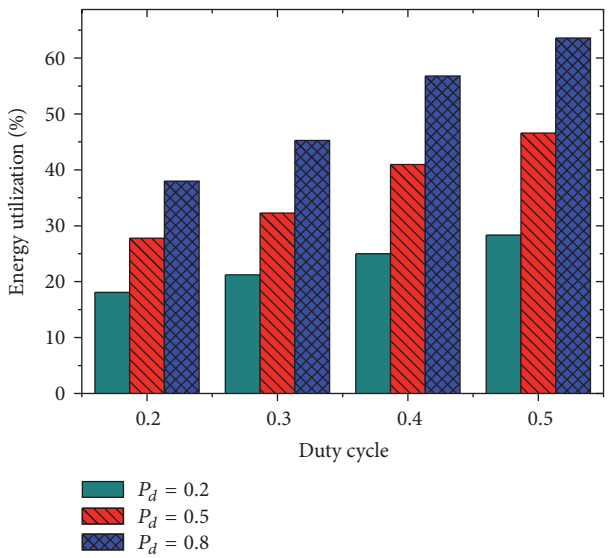

Figure 27: Energy utilization under different probability of generating data.

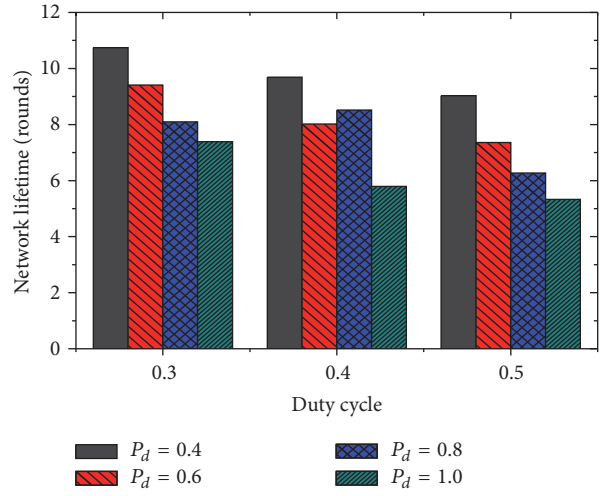

Figure 28: Network lifetime under different probability of generating data.

delay-sensitive data is greater than delay-tolerant data. From Figures 25 and 26, we can see the effectiveness of DSDR: when there are more delay-sensitive data in the network, the DSDR can transfer data to the sink quickly and has a high transmission efficiency; when there are more delay-tolerant data in the network, the DSDR can reduce energy consumption and improve network lifetime.

(2) The Probability of Data Generation. Figures 27 and 28 show the effect of the probability of data generation on network performance. When the probability is higher, the network needs to transmit more data, and the data amount each node needs to forward is greater, thus the energy consumption is more serious, and the network energy utilization is higher, but this also shortens the network lifetime. From Figure 27, we can see that the energy utilization increases with the increase of data generation rate and duty cycle. Contrary to the energy utilization, it can be seen from Figure 28 that the network lifetime is shortened as the data generation rate increases.

(3) Network Radius and Node Communication Radius. The relationship between communication radius of nodes and network radius is also an important factor that affects the performance of the network. When the communication radius of the node is larger, it means that the node can forward farther at each hop, and the number of relay hops is less.

Figures 29 and 30 show the effect of the node communication radius on the transmission delay. It can be seen that when the communication radius is greater, the number of relay hops is less and the transmission delay is smaller. Similarly, when the network radius is small, the node needs to be relayed multiple hops before its arrival to the sink, the energy

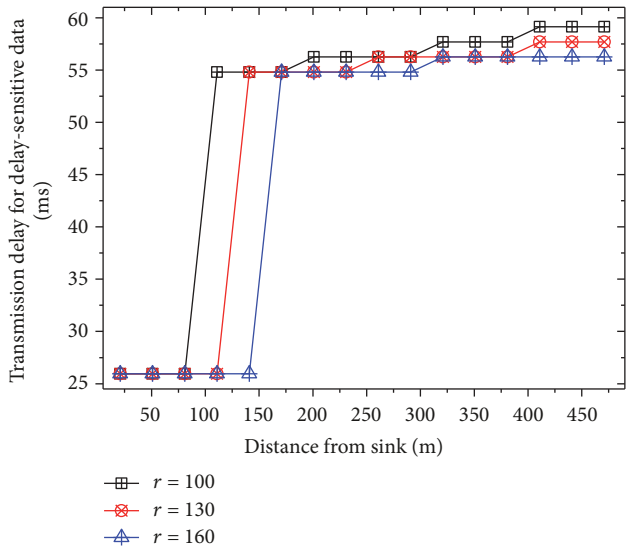

Figure 29: Transmission delay for delay-sensitive data.

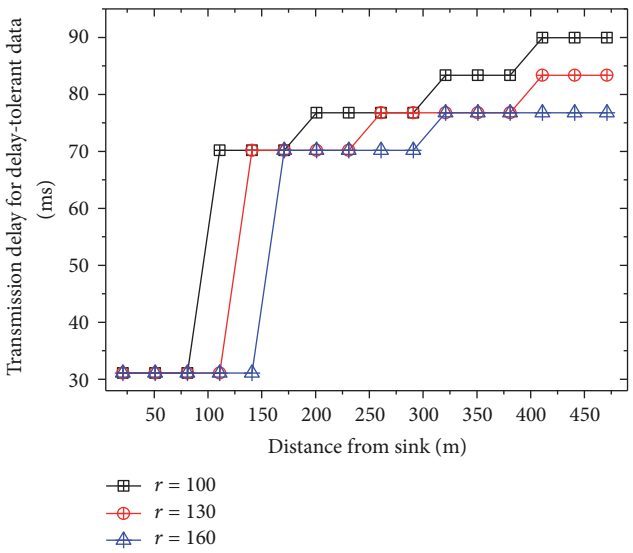

Figure 30: Transmission delay for delay-tolerant data.

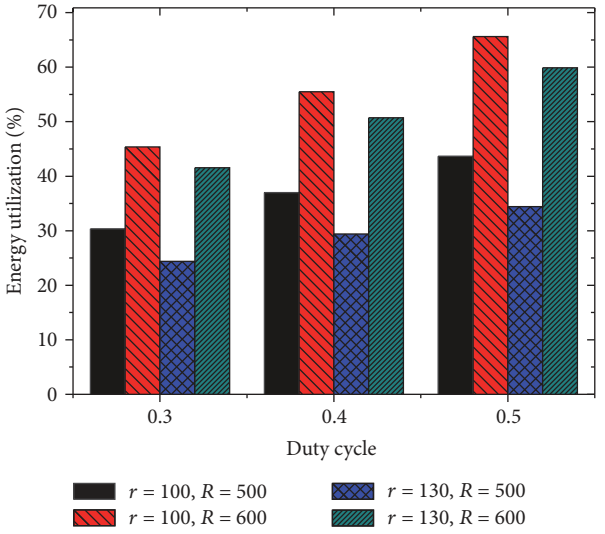

Figure 31: Energy utilization under different network radius and communication radius.

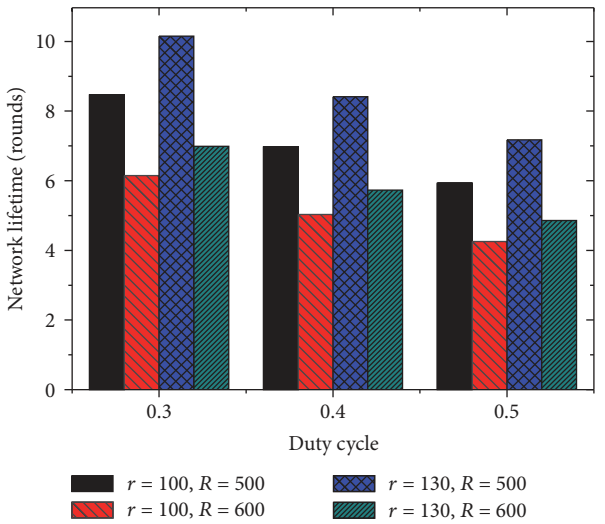

Figure 32: Network lifetime under different network radius and communication radius.

consumption is more serious, and the energy consumption directly affects the energy utilization, and also it has an impact on the network lifetime, as shown in Figures 31 and 32.

6. Conclusions and Future Work

Applications running on the same network may have different service requirements depending on the different backgrounds of their events, and the basic requirement is the transmission delay. Traditional wireless sensor networks lack intelligence and cannot dynamically select appropriate data routing according to the delay sensitivity of the data, so it cannot meet the requirements of the events. Then, a delay Differentiated Services for Data Routing scheme (DSDR) is creatively proposed in this paper, which establishes energy-efficient routing paths (E2RPs) at different locations of the network to forward data. In DSDR, data routing is intelligently selected according to the delay requirements of data. For delay-sensitive data it provides direct-forwarding method to minimize the transmission delay. For delay-tolerant data it uses wait-forwarding method and reduces redundancy by data fusion, thus to reduce network energy consumption. A comprehensive performance analysis shows that DSDR has significant advantages in terms of transmission delay and energy utilization. Compared with the general approaches, DSDR can reduce the transmission delay of delay-sensitive data by 44.31%, reduce transmission delay of delay-tolerant data by 25.65%, and improve the energy utilization by 30.61%, while also enabling the network to have a lifetime that is not less than the previous studies.

With the depth of the relevant research, the content of this paper can be extended. In this paper, we mainly study the delay differentiated services of data; in fact, the integrity of the data can also be differentiated by establishing different transmission routings in the network according to the delay and integrity requirements. Therefore, in the next working plan, we consider data integrity in the guarantee of transmission latency.

Parameters Related to Calculation

ϕ_S: Sensing duty cycle
ϕ_C: Communication duty cycle
ϵ_{Lp}: Energy consumption in low power listening
ϵ_{Td}: Energy consumption in data transmission
ϵ_{Se}: Energy consumption in event sensing
ϵ_{Rd}: Energy consumption in data receiving
$\prod_R$: Receiving data packets
$\prod_S$: Sending data packets
φ_{Rec}: Receiving data amount
φ_{Tran}: Transmitting data amount
D_{e2e}: End-to-end transmission delay
E_{dif}: Energy consumption difference
$\mathscr{R}_{e\_\mathrm{uti}}$: Energy utilization rate
$\mathscr{F}_\ell$: Network lifetime
E_{ς_i}: Energy consumed by node ς_i
N: Total number of sensor nodes
ς_i: The ith node in the network
ς_d^i: The node whose distance to the sink is i.

Conflicts of Interest

The authors declare that there are no conflicts of interest regarding the publication of this article.

Acknowledgments

This work was supported in part by the National Natural Science Foundation of China (61772554, 61379110, 61370229, and 61370178); the National Basic Research Program of China (973 Program) (2014CB046305); the National Key Technology R&D Program of China under Grant no. 2014BAH28F02; the S&T Projects of Guangdong Province under Grant nos. 2014B010103004, 2014B010117007, 2015B010110002, and 2016B010109008; and the S&T Project of Guangzhou Municipality under Grant no. 201604010054.

References

[1] J. Huang, Q. Duan, C.-C. Xing, and H. Wang, "Topology control for building a large-scale and energy-efficient internet of things," *IEEE Wireless Communications Magazine*, vol. 24, no. 1, pp. 67–73, 2017.

[2] J. Huang, Y. Meng, X. Gong, Y. Liu, and Q. Duan, "A novel deployment scheme for green internet of things," *IEEE Internet of Things Journal*, vol. 1, no. 2, pp. 196–205, 2014.

[3] J. Zhang, F. Ren, S. Gao, H. Yang, and C. Lin, "Dynamic routing for data integrity and delay differentiated services in wireless sensor networks," *IEEE Transactions on Mobile Computing*, vol. 14, no. 2, pp. 328–343, 2015.

[4] M. Zhou, M. Zhao, A. Liu, M. Ma, T. Wang, and C. Huang, "Fast and efficient data forwarding scheme for tracking mobile targets in sensor networks," *Symmetry*, vol. 9, no. 11, article 269, 2017.

[5] Q. Zhang and A. Liu, "An unequal redundancy level-based mechanism for reliable data collection in wireless sensor networks," *EURASIP Journal on Wireless Communications and Networking*, vol. 2016, article 258, 2016.

[6] X. Hu, T. H. S. Chu, V. C. M. Leung, and C. H. Ngai, "A survey on mobile social networks: Applications, platforms, system architectures, and future research directions," *IEEE Communications Surveys & Tutorials*, vol. 17, no. 3, pp. 1557–1581, 2014.

[7] T. Wang, Y. Li, G. Wang, J. Cao, M. Z. Bhuiyan, and W. Jia, "Sustainable and efficient data collection from WSNs to cloud," *IEEE Transactions on Sustainable Computing*, 2017.

[8] Z. Chen, M. Ma, X. Liu, A. Liu, and M. Zhao, "Reliability improved cooperative communication over wireless sensor networks," *Symmetry*, vol. 9, no. 10, p. 209, 2017.

[9] K. Xie, J. Cao, X. Wang, and J. Wen, "Optimal resource allocation for reliable and energy efficient cooperative communications," *IEEE Transactions on Wireless Communications*, vol. 12, no. 10, pp. 4994–5007, 2013.

[10] Y. Liu, X. Weng, J. Wan, X. Yue, H. Song, and A. V. Vasilakos, "Exploring data validity in transportation systems for smart cities," *IEEE Communications Magazine*, vol. 55, no. 5, pp. 26–33, 2017.

[11] Y. Xu, X. Chen, A. Liu, and C. Hu, "A latency and coverage optimized data collection scheme for smart cities based on vehicular ad-hoc networks," *Sensors*, vol. 17, no. 4, article 888, 2017.

[12] X. Chen, Y. Xu, and A. Liu, "Cross Layer Design for Optimizing Transmission Reliability, Energy Efficiency, and Lifetime in Body Sensor Networks," *Sensors*, vol. 17, no. 4, p. 900, 2017.

[13] A. Liu, X. Liu, Z. Tang, L. T. Yang, and Z. Shao, "Preserving Smart Sink-Location Privacy with Delay Guaranteed Routing Scheme for WSNs," *ACM Transactions on Embedded Computing Systems*, vol. 16, no. 3, pp. 1–25, 2017.

[14] Z. Chen, A. Liu, Z. Li, Y. Choi, and J. Li, "Distributed duty cycle control for delay improvement in wireless sensor networks," *Peer-to-Peer Networking and Applications*, vol. 10, no. 3, pp. 559–578, 2017.

[15] K. P. Naveen and A. Kumar, "Relay selection for geographical forwarding in sleep-wake cycling wireless sensor networks," *IEEE Transactions on Mobile Computing*, vol. 12, no. 3, pp. 475–488, 2013.

[16] H. Rasouli, Y. S. Kavian, and H. F. Rashvand, "ADCA: Adaptive duty cycle algorithm for energy efficient IEEE 802.15.4 beacon-enabled wireless sensor networks," *IEEE Sensors Journal*, vol. 14, no. 11, pp. 3893–3902, 2014.

[17] D. Gao, H. Lin, Y. Liu, and A. Jiang, "Minimizing end-to-end delay routing protocol for rechargeable wireless sensor networks," *Ad Hoc & Sensor Wireless Networks*, vol. 34, no. 1-4, pp. 77–98, 2016.

[18] Z. Su and Q. Xu, "Content distribution over content centric mobile social networks in 5G," *IEEE Communications Magazine*, vol. 53, no. 6, pp. 66–72, 2015.

[19] S. He, D.-H. Shin, J. Zhang, J. Chen, and Y. Sun, "Full-view area coverage in camera sensor networks: dimension reduction and near-optimal solutions," *IEEE Transactions on Vehicular Technology*, vol. 65, no. 9, pp. 7448–7461, 2015.

[20] G. Rajalingham, Y. Gao, Q.-D. Ho, and T. Le-Ngoc, "Quality of service differentiation for smart grid Neighbor Area Networks through multiple RPL instances," in *Proceedings of the 10th ACM Symposium on QoS and Security for Wireless and Mobile Networks, Q2SWinet 2014*, pp. 17–24, Canada, September 2014.

[21] J. Gui and K. Zhou, "Flexible adjustments between energy and capacity for topology control in heterogeneous wireless multi-hop networks," *Journal of Network and Systems Management*, vol. 24, no. 4, pp. 789–812, 2016.

[22] L. A. Villas, A. Boukerche, H. S. Ramos, H. A. B. F. De Oliveira, R. B. De Araujo, and A. A. F. Loureiro, "DRINA: A lightweight and reliable routing approach for in-network aggregation in wireless sensor networks," *IEEE Transactions on Computers*, vol. 62, no. 4, pp. 676–689, 2013.

[23] X. Chen, M. Ma, and A. Liu, "Dynamic Power Management and Adaptive Packet Size Selection for IoT in e-Healthcare," *Computers & Electrical Engineering*, 2017.

[24] Y. Xu, A. Liu, and C. Changqin, "Delay-aware program codes dissemination scheme in internet of everything, mobile information systems," *Mobile Information Systems*, vol. 2016, Article ID 2436074, 18 pages, 2016.

[25] A. Liu, X. Liu, T. Wei, L. T. Yang, S. Rho, and A. Paul, "Distributed multi-representative re-fusion approach for heterogeneous sensing data collection," *ACM Transactions on Embedded Computing Systems*, vol. 16, no. 3, Article ID 73, 2017.

[26] J. Wang, A. Liu, T. Yan, and Z. Zeng, "A resource allocation model based on double-sided combinational auctions for transparent computing," *Peer-to-Peer Networking and Applications*, pp. 1–18, 2017.

[27] Z. Su, Q. Xu, H. Zhu, and Y. Wang, "A novel design for content delivery over software defined mobile social networks," *IEEE Network*, vol. 29, no. 4, pp. 62–67, 2015.

[28] T. Li, Y. Liu, L. Gao, and A. Liu, "A cooperative-based model for smart-sensing tasks in fog computing," *IEEE Access*, vol. 5, pp. 21296–21311, 2017.

[29] A. Liu, Z. Chen, and N. N. Xiong, "An Adaptive Virtual Relaying Set Scheme for Loss-and-Delay Sensitive WSNs," *Information Sciences*, vol. 424, pp. 118–136, 2018.

[30] W. Chu, L. Wang, H. Xie, Z.-L. Zhang, and Z. Jiang, "Network delay guarantee for differentiated services in content-centric networking," *Computer Communications*, vol. 76, pp. 54–66, 2016.

[31] E. Felemban, C.-G. Lee, and E. Ekici, "MMSPEED: multipath multi-SPEED protocol for QoS guarantee of reliability and timeliness in wireless sensor networks," *IEEE Transactions on Mobile Computing*, vol. 5, no. 6, pp. 738–753, 2006.

[32] S. He, J. Chen, X. Li, X. S. Shen, and Y. Sun, "Mobility and intruder prior information improving the barrier coverage of sparse sensor networks," *IEEE Transactions on Mobile Computing*, vol. 13, no. 6, pp. 1268–1282, 2014.

[33] J. Huang, C. Xu, Q. Duan, Y. Ma, and G.-M. Muntean, "Novel end-to-end quality of service provisioning algorithms for multimedia services in virtualization-based future internet," *IEEE Transactions on Broadcasting*, vol. 58, no. 4, pp. 569–579, 2012.

[34] J. Xu, X. Liu, M. Ma, A. Liu, T. Wang, and C. Huang, "Intelligent aggregation based on content routing scheme for cloud computing," *Symmetry*, vol. 9, no. 10, 2017.

[35] Q. Xu, Z. Su, and S. Guo, "A game theoretical incentive scheme for relay selection services in mobile social networks," *IEEE Transactions on Vehicular Technology*, vol. 65, no. 8, pp. 6692–6702, 2016.

[36] X. Liu, G. Li, S. Zhang, and A. Liu, "Big program code dissemination scheme for emergency software-define wireless sensor networks," *Peer-to-Peer Networking and Applications*, pp. 1–22, 2017.

[37] L. Li, S. Li, and S. Zhao, "QoS-Aware scheduling of services-oriented internet of things," *IEEE Transactions on Industrial Informatics*, vol. 10, no. 2, pp. 1497–1507, 2014.

[38] C.-T. Cheng, H. Leung, and P. Maupin, "A delay-aware network structure for wireless sensor networks with in-network data fusion," *IEEE Sensors Journal*, vol. 13, no. 5, pp. 1622–1631, 2013.

[39] C. Dovrolis, D. Stiliadis, and P. Ramanathan, "Proportional differentiated services: delay differentiation and packet scheduling," *Computer Communication Review*, vol. 29, no. 4, pp. 109–120, 1999.

[40] Q. Liu and A. Liu, "On the hybrid using of unicast-broadcast in wireless sensor networks," *Computers & Electrical Engineering*, 2017.

[41] K. Xie, X. Wang, J. Wen, and J. Cao, "Cooperative routing with relay assignment in multi-radio multi-hop wireless networks," *IEEE/ACM Transactions on Networking*, vol. 24, no. 2, pp. 859–872, 2016.

[42] H. Xin and X. Liu, "Energy-balanced transmission with accurate distances for strip-based wireless sensor networks," *IEEE Access*, vol. 5, pp. 16193–16204, 2017.

[43] Z. Ning, X. Wang, X. Kong, and W. Hou, "A Social-aware group formation framework for information diffusion in narrowband internet of things," *IEEE Internet of Things Journal*, 2017.

[44] Z. Su, Q. Xu, M. Fei, and M. Dong, "Game theoretic resource allocation in media cloud with mobile social users," *IEEE Transactions on Multimedia*, vol. 18, no. 8, pp. 1650–1660, 2016.

[45] J. Gui, L. Hui, and N. Xiong, "A game-based localized multi-objective topology control scheme in heterogeneous wireless networks," *IEEE Access*, vol. 5, pp. 2396–2416, 2017.

[46] H. Dai, G. Chen, C. Wang, S. Wang, X. Wu, and F. Wu, "Quality of energy provisioning for wireless power transfer," *IEEE Transactions on Parallel and Distributed Systems*, vol. 26, no. 2, pp. 527–537, 2015.

[47] Y. Liu, A. Liu, S. Guo, Z. Li, Y.-J. Choi, and H. Sekiya, "Context-aware collect data with energy efficient in Cyber-physical cloud systems," *Future Generation Computer Systems*, 2017.

[48] M. Hammoudeh and R. Newman, "Adaptive routing in wireless sensor networks: QoS optimisation for enhanced application performance," *Information Fusion*, vol. 22, pp. 3–15, 2015.